GEORGIA INSTITUTE OF TECHNOLOGY
OFFICE OF CONTRACT ADMINISTRATION
SPONSORED PROJECT INITIATION

no action
ADS
OCA

Date: May 23, 1979

Project Title: Implantable Electric Field Probes in Biological Systems

Project No: E-21-658 Green card

Project Director: Dr. Glenn S. Smith

Sponsor: The University of Virginia; Charlottesville, VA 22903

Agreement Period: From 2/15/79 Until ~~2/14/81~~ April 14, 1981 (Period of Performance)

Type Agreement: Subgrant under Prime Grant No. ENG78-18273

Amount: $28,242

Reports Required: Semi-Annual Letter Reports; Final Report

Sponsor Contact Person (s):

Technical Matters	Contractual Matters (thru OCA)
Dr. T. Batchman Electrical Engineering Department University of Virginia Charlottesville, VA 22903	Mr. Stephen Maupin Grants/Contracts Specialist Office of Sponsored Programs University of Virginia P. O. Box 3901, University Station Charlottesville, VA 22903 804/924-3735

Defense Priority Rating: N/A

Assigned to: Electrical Engineering (School/Laboratory)

COPIES TO:

- Project Director
- Division Chief (EES)
- School/Laboratory Director
- Dean/Director–EES
- Accounting Office
- Procurement Office
- Security Coordinator (OCA)
- Reports Coordinator (OCA)
- Library, Technical Reports Section
- EES Information Office
- EES Reports & Procedures
- Project File (OCA)
- Project Code (GTRI)
- Other _____

CA-3 (3/76)

GEORGIA INSTITUTE OF TECHNOLOGY
OFFICE OF CONTRACT ADMINISTRATION

SPONSORED PROJECT TERMINATION

Date: April 15, 1981

Project Title: Implantable Electric Field Probes in Biological Systems

Project No: E-21-658

Project Director: Dr. Glenn S. Smith

Sponsor: The University of Virginia; Charlottesville, VA 22903

Effective Termination Date: 4/14/81

Clearance of Accounting Charges: 4/14/81

Grant/Contract Closeout Actions Remaining:

- X Final Invoice and Closing Documents
- _ Final Fiscal Report
- _ Final Report of Inventions
- _ Govt. Property Inventory & Related Certificate
- _ Classified Material Certificate
- _ Other _____

NOTE: Final Invoice must be submitted within 90 days of termination date.

Assigned to: Electrical Engineering (School/Laboratory)

COPIES TO:

Administrative Coordinator
Research Property Management
Accounting Office
Procurement Office
Research Security Services
Reports Coordinator (OCA)
Legal Services (OCA)
Library, Technical Reports
EES Research Public Relations (2)
Project File (OCA)
Other: _____

GEORGIA INSTITUTE OF TECHNOLOGY
SCHOOL OF ELECTRICAL ENGINEERING
ATLANTA, GEORGIA 30332

TELEPHONE: (404) 894-2922

SEMI-ANNUAL PROGRESS LETTER

PROJECT E-21-658

"Implantable Electric Field Probes in Biological Systems"

with

University of Virginia
(NSF Prime Grant No. ENG78-18273)

I. Progress to Date

In a miniature field probe, an electrically small dipole antenna produces a response to an incident electromagnetic field. In addition to the deisred response provided by the dipole, undesired or stray responses may result due to the coupling of the field to other components in the probe, such as the transmission line connecting the dipole with the instrumentation. For the probe to function properly, the stray response must be negligible compared to the dipoles response. When the physical size of the dipole is reduced its response is also reduced. If the stray response is unchanged, the error it produces increases with a reduction in the size of the dipole. Thus, the stray response may determine the minimum size for the dipole or probe with a given accuracy.

In this phase of the research, the stray response due to the reception of the incident electromagnetic signal by the transmission line connecting the dipole with the instrumentation is being investigated. Two methods of analysis are being used for this problem. The first

method is approximate and uses the reciprocity theorem for electromagnetic fields to determine the receiving properties of the dipole-transmission line combination from the behavior of both elements when transmitting. In the second method an integral equation is developed for the dipole-transmission line combination and this equation is solved numerically (by the method of moments) to determine the response.

The development of both methods is nearly complete and numerical calculations will soon be obtained.

II. Participation

Principal Investigator: G. S. Smith, 30% time Fall Quarter
20% time Winter Quarter

III. Documentation

None

IV. Travel

December 14, 1979, Technical Meeting
University of Virginia
(Smith)

GEORGIA INSTITUTE OF TECHNOLOGY
SCHOOL OF ELECTRICAL ENGINEERING
ATLANTA, GEORGIA 30332

TELEPHONE: (404) 894-

SEMI-ANNUAL PROGRESS LETTER

PROJECT E-21-658

"Implantable Electric Field Probes in Biological Systems"

with

University of Virginia
(NSF Prime Grant No. ENG 78-18273)

Period Covered: February 15, 1980 to August 14, 1980

I. Progress to Date

As discussed in the last progress letter, the electromagnetic signal present at the diode of the electric field probe has components that result from the reception of the incident signal by the dipole antenna and also from the reception of the incident signal by the resistive transmission line used to connect the dipole with the monitoring instrumentation. For the probe to function properly, the reception by the transmission line must be made negligible in comparison to that of the dipole.

A reduction in the size (length) of the dipole antenna to increase the spatial resolution or the frequency bandwidth of the probe will also cause a reduction in the amplitude of the signal received by the dipole. Qualitative arguments show that the reception by the two-wire transmission line decreases as the resistance per unit length of the conductors is increased and as the spacing of the conductors is decreased. Thus, for the reception by the transmission line to remain negligible as the size of the dipole is reduced, the resistance of the conductors must be increased and their spacing decreased.

As the above argument illustrates, the reception of the incident field by both the dipole antenna and the resistive transmission line influence the design of a miniature field probe. An analytical understanding of this reception is necessary if the minimum practical size for the probe is to be established and if the design of the probe is to be optimized. In the current research program, analyses are being developed to determine the reception by the dipole antenna and the transmission line of a probe with the geometry shown in Figure 1.

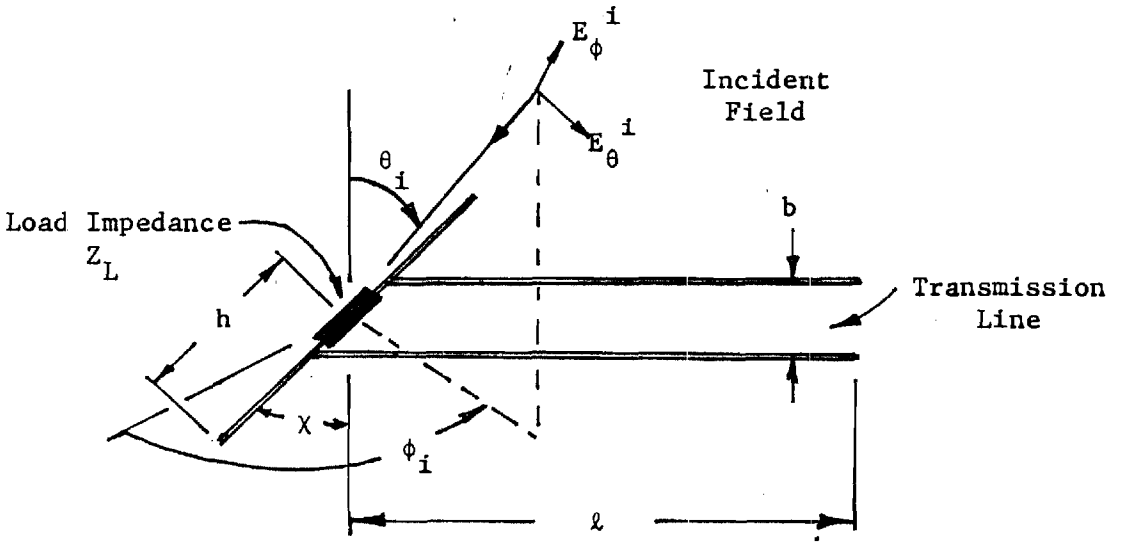

Fig. 1. Geometry of Probe

For the analysis, the electromagnetic field is a plane wave with electric field $\vec{E}^i = E_\theta^i \hat{\theta}_i + E_\phi^i \hat{\phi}_i$ incident from the direction θ_i, ϕ_i. The dipole is in the plane of the transmission line and makes angle χ with the

conductors of the line. Each conductor of the transmission line has an internal impedance per unit length $z^i = r^i + jx^i$ (Ω/m).

The structure shown in Figure 1 has been analyzed by two methods. The first method is an elementary theory that treats the reception by the dipole and the line separately. The electromagnetic coupling between the dipole and line and the end effects for the transmission line are not included. The results of this theory are simple equations that can be used in probe design. The second method is a full electromagnetic analysis of the structure by a numerical technique (the method of moments). This last approach includes the coupling between the dipole and the transmission line and the transmission line end effects, therefore, it can be used to ealuate the approximations used in the elementary theory. The formulations for both methods of analysis have been completed and numerical results are now being computed.

In addition to the theoretical analyses, limited experimental investigations are being conducted using scale model probes. The objective of the experiments is to verify the theoretical results. The model probes are scaled up versions of the miniature probes under study, i.e., models with a scale factor greater than one, and have the geometry shown in Figure 1. Typical dimensions for the probes are h = 1 cm, b = 0.5 cm and ℓ = 15 cm. In the experiment, the field pattern of the probe is measured as a function of the angle θ_i in the plane $\phi_i = 0,\pi$. The incident electric field is linearly polarized in the $\hat{\theta}$ direction ($\vec{E}^i = E_\theta^i \hat{\theta}_i$). Both conducting (copper) and highly resistive (carbon filled Teflon) conductors have been used for the transmission line.

A typical meausred field pattern for a dipole normal to the transmission line, $\chi = 90^\circ$, is shown in Figure 2. The conductors of the

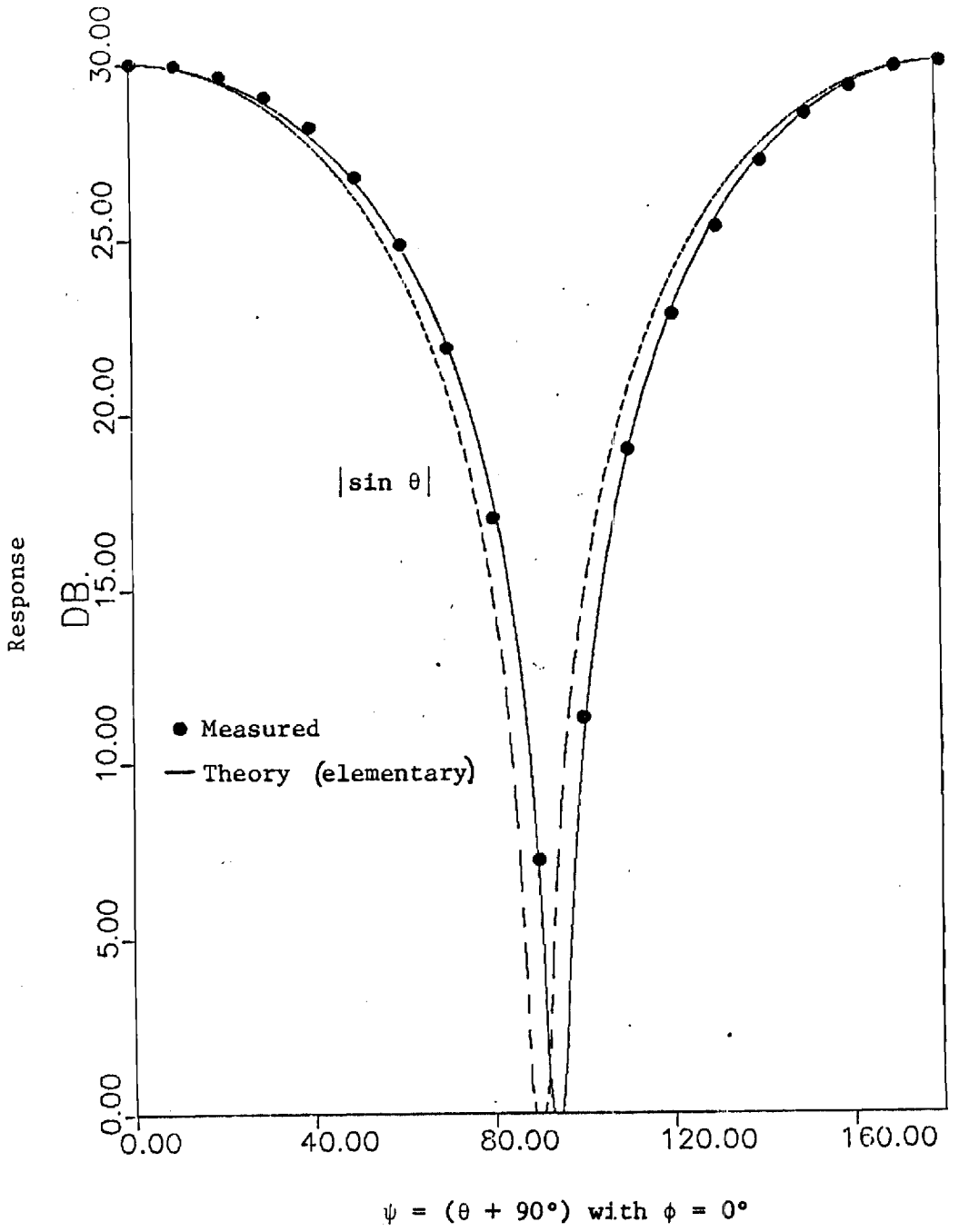

Fig. 2. Field pattern for probe with highly resistive transmission line.

transmision line for this example had a high resistance per unit length, $r^i \approx 65$ KΩ/m. The reception by the transmission line is seen to cause the pattern to depart from that of the dipole, $|\sin\theta|$, particularly in the region near the nulls. The pattern computed from the elementary theory is also shown in Figure 2 and is seen to be in good agreement with the measured results. For this case, the pattern obtained from the numerical analysis is almost identical to that for the elementary theory.

During the remainder of the period of the grant (August 15, 1980 to February 14, 1981), the research will include the following tasks.

1. The numerical analysis will be used to study the coupling between the dipole and the transmission line when these elements are not normal to each other, i.e., $\chi \neq 90$ in Figure 1.
2. The effect of an unbalance in the resistance of the conductors of the transmission line (unequal resistances per unit length in the two conductors) on the field pattern will be considered.
3. The perturbation produced by the scattering of the incident field by the transmission line will be examined and its reduction by resistive loading evaluated.

II. Participation

Principal Investigators: G. S. Smith, 30% time Spring Quarter
33% time Summer Quarter

III. Documentation

A paper describing the elementary analysis and experimental results is in preparation.

IV. Travel

None

FINAL TECHNICAL REPORT (E–21–658)

ANALYSIS OF MINIATURE ELECTRIC FIELD PROBES WITH RESISTIVE TRANSMISSION LINES

By

Glenn S. Smith

Prepared for

UNIVERSITY OF VIRGINIA
CHARLOTTESVILLE, VA 22903

(Subgrant under National Science Foundation
Prime Grant No. ENG78–18273)

April 1981

GEORGIA INSTITUTE OF TECHNOLOGY
SCHOOL OF ELECTRICAL ENGINEERING
ATLANTA, GEORGIA 30332

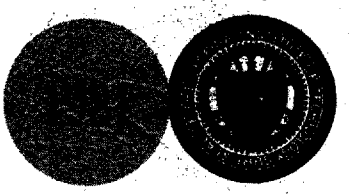

ANALYSIS OF MINIATURE ELECTRIC FIELD PROBES WITH RESISTIVE TRANSMISSION LINES

by

Glenn S. Smith
School of Electrical Engineering
Georgia Institute of Technology
Atlanta, Georgia 30332

April 1981
Final Technical Report (E-21-658)

Prepared for

UNIVERSITY OF VIRGINIA
Charlottesville, Virginia 22903

Subgrant under
National Science Foundation
Prime Grant No. ENG78-18273

INTRODUCTION

In March of 1978 a proposal entitled "Subminiature Implantable Electric Field Probes for Microwave Dosimetry in Biological Systems" was submitted to the National Science Foundation (NSF) by the University of Virginia (UVA). The proposal was a collaborative effort between the Department of Electrical Engineering at the University of Virginia, the School of Electrical Engineering at the Georgia Institute of Technology, and the U.S. Bureau of Radiological Health. A grant was subsequently awarded to UVA by NSF for the period February 1979 to July 1981, and a subgrant was made to Georgia Tech by UVA. This document is the final technical report for that subgrant.

The effort of Georgia Tech on this grant was twofold.

i. Georgia Tech provided theoretical support for the design and fabrication of subminiature field probes at UVA. This interaction occurred through telephone conversations and at technical meetings held at the University of Virginia, the Bureau of Radiological Health, Rockville, MD, and at Georgia Tech.

ii. The theoretical analysis for the miniature field probe was extended by considering, in detail, the effect of the resistive transmission line on the performance of the probe. This analysis produced information that can be used in the design and optimization of future probes.

The remainder of this report is the manuscript for a paper that describes the research performed under item (ii) above. This manuscript has been submitted for publication in a technical journal.

ANALYSIS OF MINIATURE ELECTRIC FIELD PROBES WITH RESISTIVE TRANSMISSION LINES

Glenn S. Smith, Senior Member, IEEE

Abstract

The miniature dipole probe is a useful tool for measuring the electric field at high radio and microwave frequencies. A common design for the probe consists of an electrically short dipole antenna with a diode across its terminals; a resistive parallel-wire transmission line transmits the detected signal from the diode to the monitoring instrumentation. The high resistance per unit length of the transmission line reduces the direct reception of the incident field by the line and also reduces the scattering of the incident field by the line. In addition, the resistive transmission line serves as a low-pass filter in the detection process. In this paper, the effect of the resistive transmission line on the operation of the miniature field probe is analyzed. Specifically, the reception of the incident signal by the transmission line is compared with that of the dipole. The scattering of incident signal by the transmission line is studied by means of the scattering cross section, and the limitation imposed on the measurement of amplitude modulated signals by the low-pass filtering by the resistive line is examined. The results of the theoretical analysis are presented as simple formulas which are useful in the design and optimization of the probe. The theoretical results are shown to be in good agreement with measurements.

This work was supported in part by the National Science Foundation under Grant ENG78-18273 through a subgrant to Georgia Tech from the University of Virginia, Charlottesville, VA.

The author is with the School of Electrical Engineering, Georgia Institute of Technology, Atlanta, GA.

I. INTRODUCTION

In many practical applications of electromagnetism at high radio and microwave frequencies, an accurate measurement of the electric field in free space or in a material medium is required. Examples are the calibration of electromagnetic shielded rooms and anechoic chambers, measurement of the near field of transmitting antennas, and the sensing of fields in and around transmission lines and waveguides. In addition, the recent interest in the biological effects of nonionizing electromagnetic radiation has created a need to measure the electric field in free space for hazard assessment of emissions from devices, such as microwave ovens, and in biological tissue or simulated tissue to provide dosimetry for controlled bioelectromagnetic experiments.

The electrically short receiving dipole antenna is ideally suited to this measurement, because the voltage produced at its terminals is proportional to the component of the incident electric field that is parallel to its axis. With reference to Fig. 1, the terminal voltage V is

$$V = K_e \vec{E}^i \cdot \hat{z} , \tag{1}$$

where K_e is the constant of proportionality. For a practical probe, a connection that does not perturb the measurement of the electric field must be made between the dipole and the instrumentation that monitors the voltage V. A number of dipole probes have been constructed using the basic connection shown schematically in Fig. 1. The operation of this probe is fairly simple. For an amplitude modulated incident field, the dipole produces an amplitude modulated oscillating voltage across the diode at

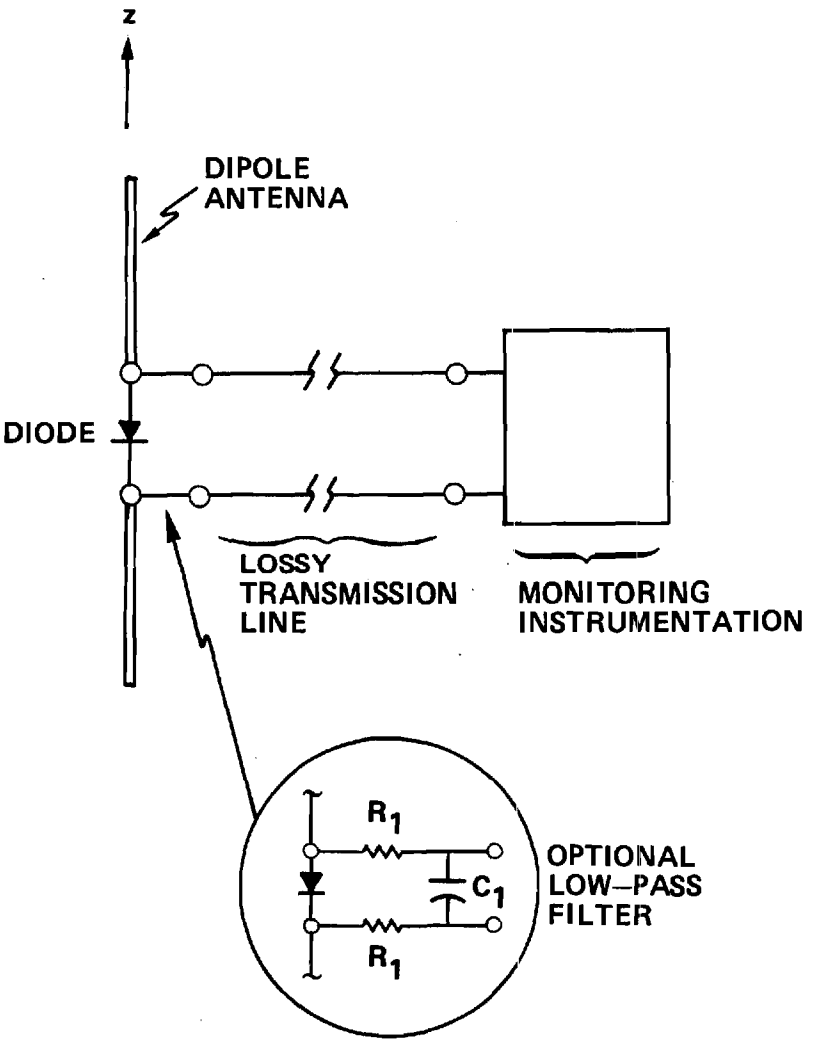

Figure 1. Dipole Receiving Probe.

its terminals. When the diode is operating in its square-law region, a current proportional to the square of the modulating signal is also developed at the diode. This current is passed through the low-pass filter formed by the lossy transmission line to the monitoring instrumentation. Thus, a signal proportional to the square of the amplitude modulation on the incident field is measured. The high resistance per unit length of the lossy transmission line reduces the signal received directly by the line and transmitted to the diode; it also reduces the scattering of the incident field by the transmission line. In some probe designs, an additional discrete-element low-pass filter is placed between the diode and the transmission line as the insert in Fig. 1 shows.

The transmission lines for early versions of this probe were constructed from very thin metallic wire with a typical resistance per unit length being 0.1 - 1 kΩ/m [1], [2]. Later versions used a "semiconducting" line developed by the U.S. National Bureau of Standards (NBS) [3]. This line is formed from polytetraflouroethylene (Teflon) impregnated with finely divided carbon black; the resistance per unit length for a 0.76 mm diameter filament is about 65.6 kΩ/m.* Typical lengths for the dipoles of these probes were 2h = 1.0 - 5.0 cm. The miniature field probes recently developed for biological applications have dipoles which are much smaller in length, 2h = 1.5 - 3.0 mm, [4]-[7]. Both electrical and biological considerations require the dipoles to be at least this small. The conductors of the transmission lines for these miniature probes are formed by depositing a thin film of a metallic alloy on a dielectric substrate; a typical resistance per unit length being 1 - 10 MΩ/m. Current interest

*This material is now commercially produced under the trade name Conductive Fluorsint by the Polymer Corporation, Reading, PA 19603.

is in utilizing the technology of microwave integrated circuits to produce even smaller dipole probes ($2h \simeq 0.5$ mm) for use in in vivo bioelectromagnetic dosimetry. When these probes are fully developed, they will have many applications in addition to those in the area of bioelectromagnetics. The design and fabrication of the lossy transmission lines for these very small probes is critical, particularly if the performance of the combination of the dipole, diode and transmission line is to be optimized. The empirical procedures used in the past may not be sufficient for this purpose.

It is the purpose of this paper to present theoretical electromagnetic analyses, supported by experimentation, for the combination of the electrically short dipole and lossy transmission line. Specificately, i) the direct reception of the incident signal by the transmission line is evaluated and compared with that for the dipole, ii) the scattering of the incident signal by the transmission line is studied by formulating the scattering cross section for the line, and iii) the behavior of the lossy line as a low-pass filter is examined. The results of the analyses are presented as simple formulas that can be used for probe design and optimization.

Only the single dipole with a lossy transmission in free space is examined. Methods for combining three dipoles to obtain an isotropic response and the special techniques, such as insulating the dipole, that are used to improve the response of the probe when immersed in a material medium are discussed in the literature [4]-[11].

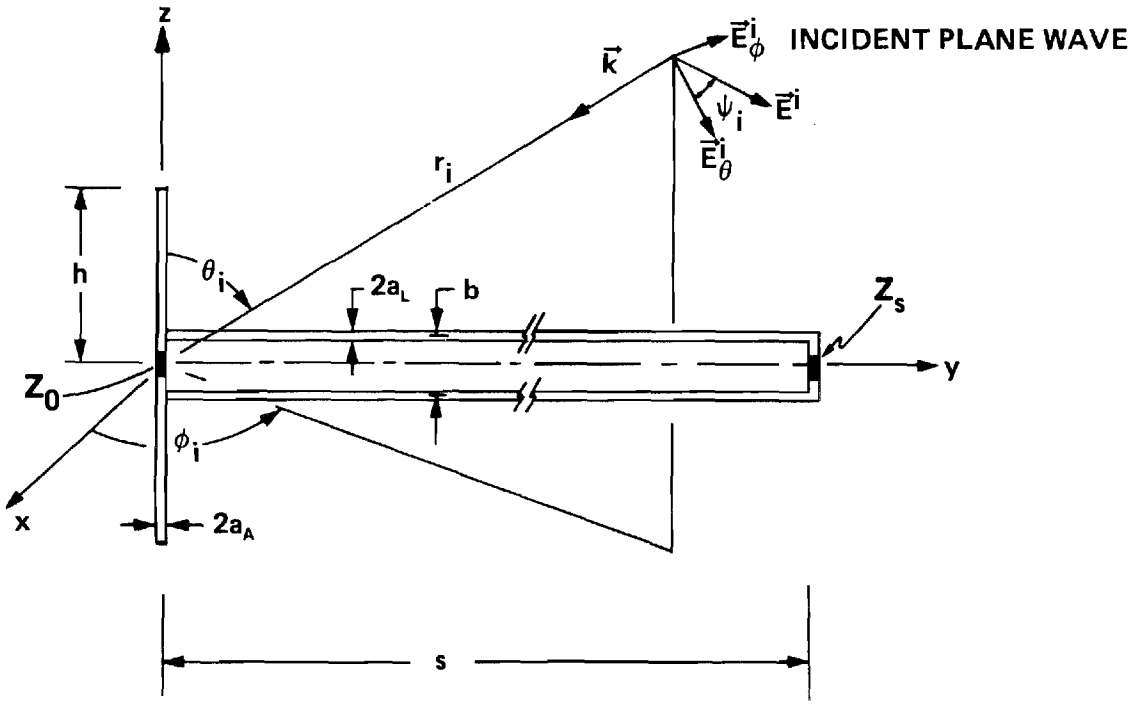

Figure 2. Dipole With Transmission Line in Incident Plane-Wave Field.

II. FORMULATION OF THE PROBLEM

Figure 2 shows the model used in the analysis for electric field probe. The dipole and transmission line are orthogonal; the axis of the dipole is parallel to the z axis and the axis of the transmission line is parallel to the y axis. The dipole has half length h and conductor radius a_A, while the transmission line has length s, conductor radius a_L and conductor spacing b. Lumped impedances Z_0 and Z_s (admittances Y_0 and Y_s) are connected at the ends of the transmission line, y=0 and y=s, respectively. In an actual probe, these elements would represent the linear high-frequency impedance of the diode and the input impedance of the monitoring instrumentation. Note that the discrete element low-pass filter in Fig. 1 is not included in the model, but it can be added easily if needed. The incident signal is a linearly polarized electromagnetic plane wave propagating in the direction specified by the angles θ_i, ϕ_i with the electric field

$$\vec{E}^i(\vec{r},\omega) = \vec{E}^i_\theta + \vec{E}^i_\phi = E^i(\cos\psi_i\hat{\theta}_i + \sin\psi_i\hat{\phi}_i)e^{-j\vec{k}\cdot\vec{r}}, \qquad (2)$$

where

$$\vec{k}\cdot\vec{r} = -\beta_o(x\sin\theta_i\cos\phi_i + y\sin\theta_i\sin\phi_i + z\cos\theta_i). \qquad (3)$$

A complex harmonic time dependence $e^{j\omega t}$ is assumed, and $\beta_o = \omega\sqrt{\mu_o\varepsilon_o}$ is the propagation constant for free space.

The incident wave produces currents in the dipole and in the transmission line. The current in the transmission line can be split into two

components: the differential mode current I_{DM}, which is equal in amplitude in the two conductors, but opposite in direction, and the common mode current I_{CM}, which has equal amplitude and the same direction in both conductors, see Fig. 3. The differential mode current I_{DM} goes through the terminal impedances Z_0 and Z_s and is responsible for the direct reception of the incident signal by the transmission line; the common mode current is zero in the terminations. The common mode current, however, is the source of the scattered electromagnetic field for the transmission line. The scattered field can produce currents in nearby objects, and these, in turn, can produce a secondary field received by the dipole or transmission line, see Fig. 3. Thus, the currents I_{DM} and I_{CM} are the sources of two errors produced in the measurement, viz, the direct reception of the incident signal by the transmission line, and the scattering of the incident signal by the transmission line that can result in the reception of an erroneous signal by the probe.

In the study of the combination of the dipole and transmission line, the reception by the transmission line, i.e., the differential mode current $I_{DM}(y=0)$ in the impedance Z_0, is calculated and compared to the reception by the dipole antenna, i.e., the antenna current I_A $(z=0)$ in the impedance Z_0. The degradation of the receiving pattern for the dipole by the transmission line is then examined. The effect of the scattering of the incident wave by the transmission line on the reception by the dipole cannot be completely assessed unless a description of all objects near the probe is provided. A measure of the effect, however, can be obtained by considering the general scattering properties of the transmission line. This is done by formulating the backscattering cross section for normal

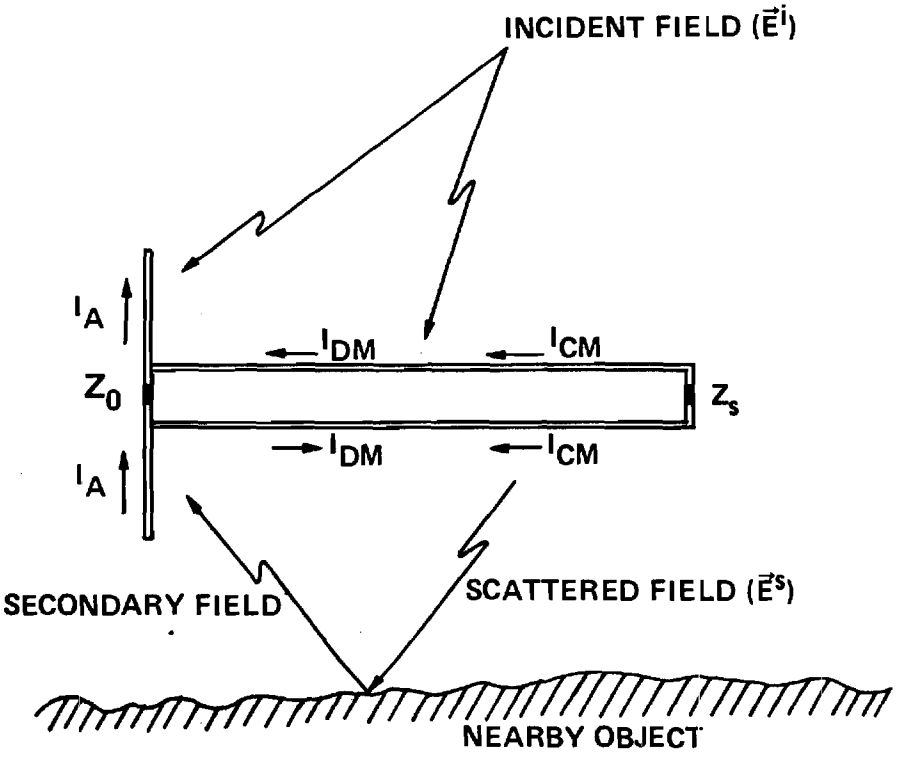

Figure 3. Schematic Diagram Showing Reception of Incident Signal.

incidence ($\theta_i = 0$, $\phi_i = \pi/2$, $\psi_i = 0$) and the total scattering cross section.

In the analysis the electromagnetic coupling between the dipole and the orthogonal transmission line is ignored, and the only interaction considered between these elements is at their connection.

III. RECEPTION OF THE INCIDENT WAVE

The reception of the incident signal by the combination of the dipole and the transmission line is analyzed using the Norton equivalent circuit shown in Fig. 4. In this circuit, the current generators I_{ASC} and I_{LSC} are the currents that would be produced by the incident field in a short circuit at the terminals of the dipole and transmission line, respectively, and the admittances Y_A and Y_L are those for the driven dipole and the driven transmission line. For an electrically short dipole ($\beta_o h << 1$) the circuit elements are

$$I_{ASC} \approx -hE^i \cos\psi_i \sin\theta_i Y_A \ , \tag{4}$$

$$Y_A \approx j\pi\beta_o h/\zeta_o[\ell n(h/a_A)-1] \ , \tag{5}$$

where terms of order $(\beta_o h)^2$ or less have been ignored, and $\zeta_o = \sqrt{\mu_o \varepsilon_o}$ is the impedance of free space [10]. The input admittance for the transmission line is simply

$$Y_L = Y_c \left[\frac{Y_s + jY_c \tan(k_L s)}{jY_s \tan(k_L s) + Y_c}\right] \ , \tag{6}$$

where the complex wavenumber k_L and characteristic admittance Y_c (impedance Z_c) are expressed in terms of the series impedance per unit length z_L and shunt admittance per unit length y_L,

$$k_L = \beta_L - j\alpha_L = \sqrt{-z_L y_L} \ , \tag{7}$$

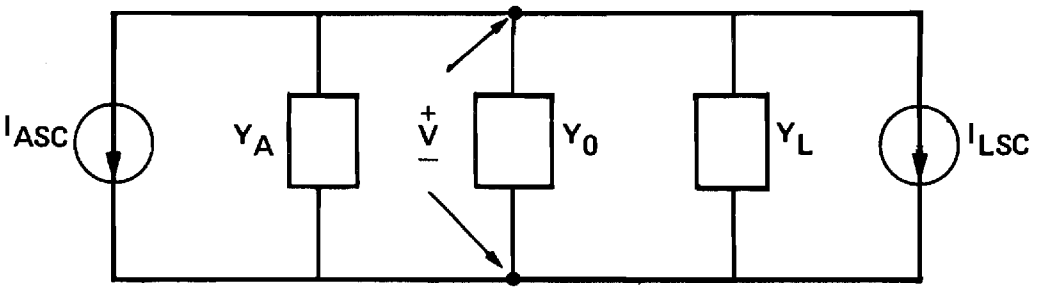

Figure 4. Norton Equivalent Circuit for Dipole–Transmission Line Reception.

$$Y_c = 1/Z_c = \sqrt{y_L/z_L} \ . \tag{8}$$

The series impedance per unit length is the sum of the internal impedance per unit length of the conductors $2z^i$ and the impedance of the external inductance per unit length ℓ^e

$$z_L = 2z^i + j\omega\ell^e = 2r^i + j\omega(2\ell^i + \ell^e) \ , \tag{9}$$

and the shunt admittance per unit length is the sum of the conductance per unit length and the admittance of the capacitance per unit length

$$y_L = g + j\omega c \ . \tag{10}$$

Note that the internal impedance per unit length of each conductor is z^i, requiring the factor of two in the loop impedance per unit length (9). It remains to determine the equivalent current generator for the transmission line I_{LSC} by analyzing the excitation of the line by the incident field.

The effect of the incident electromagnetic field on the transmission line is equivalent to a distributed series voltage source and a distributed shunt current source [12], [13], see Figure 5. For a general incident field $\vec{E}^i(x,y,z)$, $\vec{B}^i(x,y,z)$, the equivalent voltage and current sources per unit length of the line are

$$V_s(y) = j\omega \int_{-b/2}^{b/2} B_x{}^i(0,y,z)dz \tag{11}$$

and

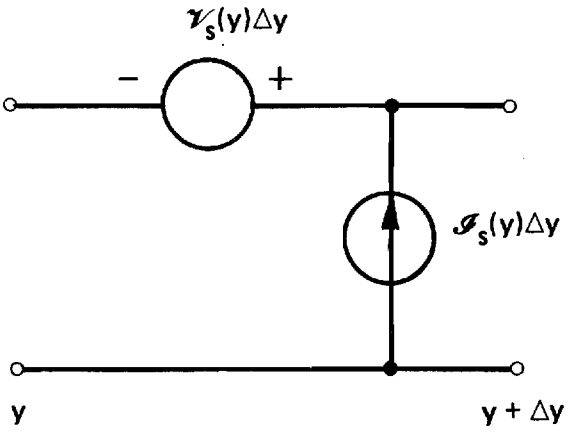

Figure 5. Equivalent Voltage and Current Sources for a Length Δy of the Transmission Line.

$$I_s(y) = -y_L \int_{-b/2}^{b/2} E_z^i(0,y,z)dz \ . \tag{12}$$

These sources appear on the right-hand side of the transmission line equations for the differential mode voltage and current

$$\frac{\partial V_{DM}(y)}{\partial y} + z_L I_{DM}(y) = V_s(y) \ , \tag{13}$$

$$\frac{\partial I_{DM}(y)}{\partial y} + y_L V_{DM}(y) = I_s(y) \ . \tag{14}$$

After combining (11)-(14) and using Maxwell's equations, the following partial differential equations of the second order are obtained for the voltage and the current on the transmission line

$$\frac{\partial^2 V_{DM}(y)}{\partial y^2} + k_L^2 V_{DM}(y) = y_L 2z^i \int_{-b/2}^{b/2} E_z^i(0,y,z)dz + j\omega \int_{-b/2}^{b/2} \frac{\partial B_y^i(0,y,z)}{\partial x} dz \ , \tag{15}$$

$$\frac{\partial^2 I_{DM}(y)}{\partial y^2} + k_L^2 I_{DM}(y) = y_L [E_y^i(0,y,b/2) - E_y^i(0,y,-b/2)] \ . \tag{16}$$

The solution of the differential system consisting of (15), (16) and the boundary conditions $V_{DM}(0) = -Z_0 I_{DM}(0)$, $V_{DM}(s) = Z_s I_{DM}(s)$ is straightforward [12], [13]. Specifically, the solution for the current at the left termination of the line, y=0, is

$$I_{DM}(0) = \{ [j\bar{Z}_s \sin k_L s + \cos k_L s] \int_{-b/2}^{b/2} E_z^i(0,0,z)dz - \int_{-b/2}^{b/2} E_z^i(0,s,z)dz$$

$$- \int_0^s [E_y^i(0,y,b/2)-E_y^i(0,y,-b/2)][j\bar{Z}_s \sin k_L(y-s)-\cos k_L(y-s)]dy\}/Z_c D \ , \tag{17}$$

where

$$D = j(1 + \bar{Z}_0\bar{Z}_s)\sin k_L s + (\bar{Z}_0 + \bar{Z}_s)\cos k_L s \ , \tag{18}$$

and the normalized impedance $\bar{Z}$ (admittance $\bar{Y}$) is $\bar{Z} = Z/Z_c$ ($\bar{Y} = Y/Y_c$). When the incident field (2) is substituted into (17), the inequality $\beta_o b << 1$ used, and the integrals evaluated, the current becomes

$$I_{DM}(0) = (E^i b/Z_c)\{\cos \theta_i[(\cos k_L s - e^{j\beta_o s \sin \theta_i \sin \phi_i})(\sin \theta_i \sin \phi_i$$

$$+ \bar{k}_L\bar{Z}_s) + j \sin k_L s(\bar{Z}_s \sin \theta_i \sin \phi_i + \bar{k}_L)]$$

$$[\cos \theta_i \sin \phi_i \cos \psi_i + \cos \phi_i \sin \psi_i]/(\bar{k}_L^2 - \sin^2\theta_i \sin^2\phi_i)$$

$$- \sin \theta_i[j\bar{Z}_s \sin k_L s + \cos k_L s - e^{j\beta_o s \sin \theta_i \sin \phi_i}]$$

$$\cos \psi_i\}/D \ , \tag{19}$$

where $\bar{k}_L = k_L/\beta_o$. The current generator I_{LSC}, which appears in the Norton equivalent circuit of Fig. 4, is determined by setting Z_0 equal to zero in (19)

$$I_{LSC} = I_{DM}(0)\Big|_{Z_0 = 0} \ . \tag{20}$$

With the values of elements in the equivalent circuit of Fig. 4 given by (4)-(6) and (20), the oscillating voltage V across the terminals of the load impedance Z_0 (admittance Y_0) is determined

$$V = -(I_{ASC} + I_{LSC})/(Y_A + Y_L + Y_0) \ . \tag{21}$$

From this equation it is seen that the relative reception of the incident field by the dipole and the transmission line can be evaluated by comparing the two components of the total short-circuit current $I_{TSC} = I_{ASC} + I_{LSC}$. For the special case of interest, the high loss per unit length of the transmission line introduces the inequality

$$\left| e^{-jk_L s} \right| = e^{-\alpha_L s} << 1 \ , \tag{22}$$

which simplifies greatly the expressions for the current I_{LSC} and the admittance Y_L,

$$I_{LSC} \approx (E^i b/Z_c)[\cos \theta_i(\cos \theta_i \sin \phi_i \cos \psi_i + \cos \phi_i \sin \psi_i)/$$

$$(\bar{k}_L - \sin \theta_i \sin \phi_i) - \sin \theta_i \cos \psi_i] \ , \tag{23}$$

$$Y_L \approx Y_c \ . \tag{24}$$

After combining (4) and (23), the total short-circuit current becomes

$$I_{TSC} \approx \frac{-j\pi\omega\varepsilon_o h^2 E^i}{\ell n(h/a_A) - 1}\{\sin \theta_i \cos \psi_i$$

$$- \chi [\cos \theta_i (\cos \theta_i \sin \phi_i \cos \psi_i + \cos \phi_i \sin \psi_i)/$$

$$(1 - \sin \theta_i \sin \phi_i / \bar{k}_L) - \bar{k}_L \sin \theta_i \cos \psi_i] \} , \qquad (25)$$

where the parameter χ is

$$\chi = \frac{\ell n(h/a_A) - 1}{\pi} (b/h)(\zeta_o / z_L h) . \qquad (26)$$

Note that after the use of (22), the current I_{TSC} is independent of the length s of the transmission line and the load impedance Z_s.

Additional simplification of (25) is possible if assumptions are made concerning the impedance and admittance per unit length of the transmission line. For a line with negligible conductance per unit length $g \approx 0$ and a high resistance per unit length $2r^i >> \omega (2\ell^i + \ell^e)$,

$$z_L \approx 2r^i , \qquad y_L \approx j\omega c , \qquad (27)$$

which makes

$$\bar{k}_L \approx \sqrt{-j\omega 2r^i c} \, / \beta_o = \sqrt{r^i / \omega \ell^e} \, (1-j) , \qquad (28a)$$

thus,

$$|\bar{k}_L| >> 1 . \qquad (28b)$$

With these results (25) becomes

$$I_{TSC} \approx \frac{-j\pi\omega\varepsilon_o h^2 E^i}{\ell n(h/a_A) - 1} \{F_A(\theta_i) \cos\psi_i$$

$$- \chi [F_{L1}(\theta_i,\phi_i)\cos\psi_i + F_{L2}(\theta_i,\phi_i)\sin\psi_i$$

$$- \bar{k}_L F_A(\theta_i)\cos\psi_i]\} \quad , \tag{29}$$

where

$$F_A(\theta_i) = \sin\theta_i \tag{30a}$$

$$F_{L1}(\theta_i,\phi_i) = \cos^2\theta_i \sin\phi_i \tag{30b}$$

$$F_{L2}(\theta_i,\phi_i) = \cos\theta_i \cos\phi_i \quad , \tag{30c}$$

and

$$\chi \approx \frac{\ell n(h/a_A) - 1}{\pi} (b/h)(\zeta_o/2r^i h) \quad . \tag{31}$$

The first term in the braces in (29) results from the reception of the incident field by the electrically short dipole antenna, the remainder, i.e., the terms with the coefficient χ, is due to the reception by the transmission line. A careful examination of these terms will indicate the effect of the transmission line on the response of the electric field probe. The response of the dipole antenna, specified by the function $F_A(\theta_i)$, is to the $\hat{\theta}_i$ component of the incident electric field, and it has the familiar figure-eight shaped polar field pattern shown in Fig. 6. The response of the transmission line has three terms, the last of these has

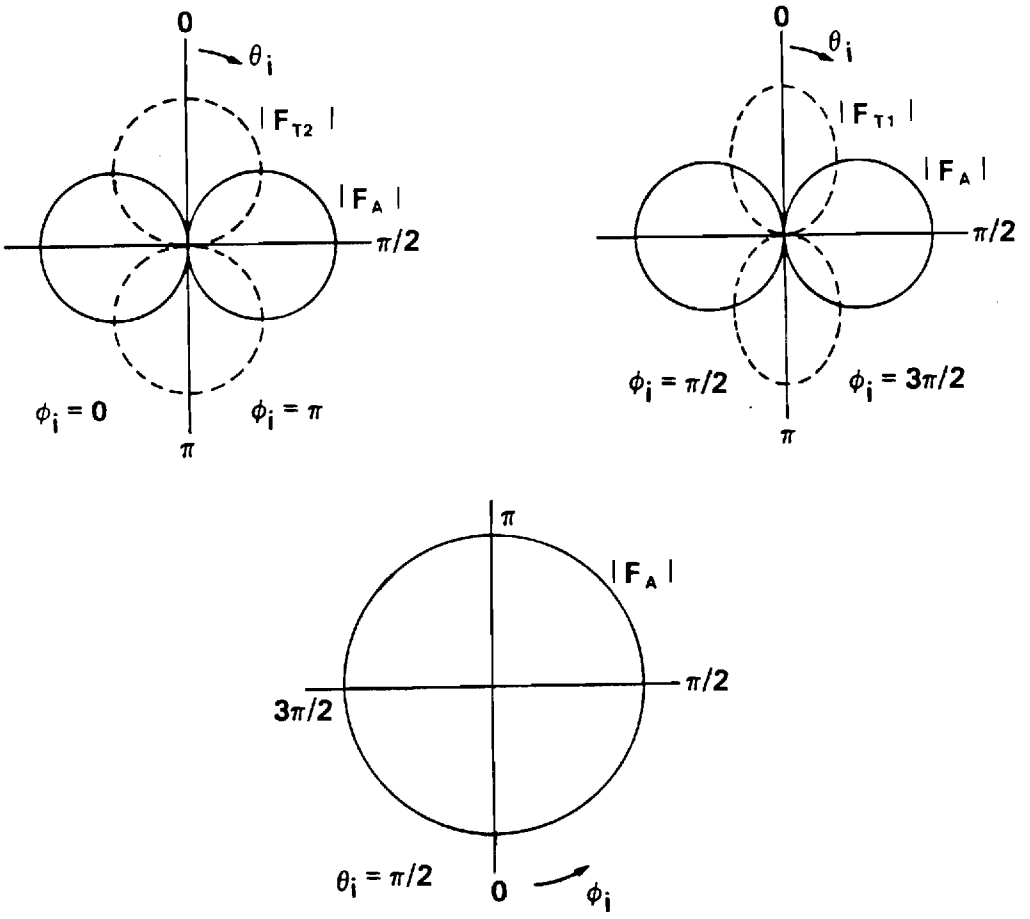

Figure 6. Polar Field Patterns in Principal Planes for Functions $F_A(\theta_i, \phi_i)$, $F_{T1}(\theta_i, \phi_i)$ and $F_{T2}(\theta_i, \phi_i)$.

the same form as the response for the dipole, $F_A(\theta_i)$, and simply contributes to the desired response for the probe. The other two terms are responses to the $\hat{\theta}_i$ and $\hat{\phi}_i$ components of the incident field and are proportional to the functions $F_{L1}(\theta_i,\phi_i)$ and $F_{L2}(\theta_i,\phi_i)$, respectively. The former causes the pattern for the probe to deviate from that for the dipole, particularly in the vicinity of the nulls, and the latter causes the probe to respond to an electric field orthogonal to the dipole. Polar patterns for the functions $F_{L1}(\theta_i,\phi_i)$ and $F_{L2}(\theta_i,\phi_i)$ in the principal planes are shown in Fig. 6.

For purposes of discussion, it is convenient to combine the terms proportional to $F_A(\theta_i,\phi_i)$ in (29) and introduce the normalized current I_{TSC},

$$\bar{I}_{TSC} = I_{TSC}/\{-j\omega\varepsilon_o h^2(1 + \bar{k}_L\chi)E^i/[\ell n(h/a_A)-1]\}$$

$$= F_A(\theta_i)\cos\psi_i - \bar{\chi}[F_{L1}(\theta_i,\phi_i)\cos\psi_i$$

$$+ F_{L2}(\theta_i,\phi_i)\sin\psi_i] \quad , \tag{32}$$

where

$$\bar{\chi} = \chi/(1 + \bar{k}_L\chi) = \chi/\{1 + (b/h)(1/k_L h)[\ell n(h/a_A)-1]/\pi\} \quad . \tag{33}$$

The deviation of the normalized response of the probe (32) from that of the ideal dipole, the error in the response, is simply proportional to the complex parameter $\bar{\chi}$ (33). The magnitude of this parameter is always less than the real parameter χ (31), $|\bar{\chi}| \leq \chi$, and for many practical designs

$|\bar{k}_L\chi| << 1$, so that $\bar{\chi} \approx \chi$. Therefore, the real parameter χ is a useful measure of the error in the response of the probe. Note that the product of the dimensionless ratios (b/h) and $(\zeta_o/r^i h)$ appears in the expression for χ. Thus, if the length h of the dipole in a probe is to be reduced by a factor ξ without increasing the error (χ) in the response, the spacing between the conductors of the transmission line must be decreased by the factor ξ and their resistance per unit length must be increased by the factor $1/\xi$. Alternatively, only the spacing or the resistance need be changed, but then by the factors ξ^2 and $(1/\xi)^2$, respectively. Note that χ is not a function of the frequency when the resistance per unit length r^i is frequency independent.

To illustrate the error introduced in the response of the probe by the transmission line, rectangular field patterns are shown in Fig. 7 for a probe with the parameter $\chi = 0.3$ ($|\bar{k}_L\chi| << 1$). The reception by the transmission line is seen to cause the pattern of the probe in the plane $\phi_i = \pi/2, 3\pi/2$ for an incident field $\vec{E}_\theta^{\,i}$ to deviate from that of the ideal dipole $|\sin\theta_i|$. The width of the lobe in the half plane $\phi_i = \pi/2$ is decreased, while the width of the lobe in the half plane $\phi_i = 3\pi/2$ is increased. The nulls in the pattern are shifted by approximately the amount

$$\Delta\theta \approx (\sqrt{1 + 4\chi^2} - 1)/2\chi \ , \tag{34}$$

which for this example is about 16.1°. In the plane $\phi_i = 0,\pi$, the pattern of the probe for an incident field $\vec{E}_\theta^{\,i}$ is the same as that of an ideal dipole; however, there is a response to an incident field $\vec{E}_\phi^{\,i}$ that does not exist for the ideal dipole.

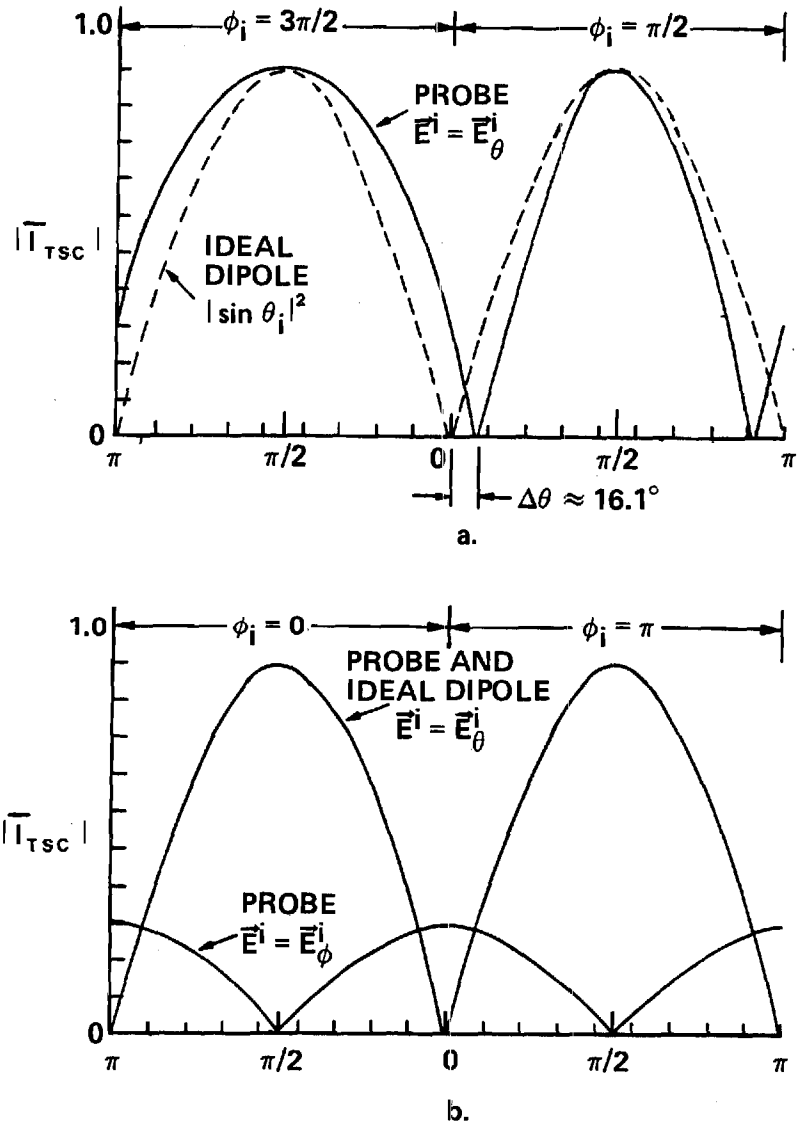

Figure 7. Rectangular Field Patterns in Principal Planes for Probe With Parameter $\chi = 0.3$, a. $\phi_i = \pi/2, 3\pi/2$, b. $\phi_i = 0, \pi$.

IV. SCATTERING OF THE INCIDENT WAVE

The currents produced in the dipole antenna and the transmission line by the incident field are the sources of the secondary or scattered field. With reference to Fig. 3, the current I_A is the souce of the scattered field for the dipole antenna. At distances from the transmission line that are large compared to the spacing of the conductors b, the field of the common mode current I_{CM} is much greater than that of the differential mode current I_{DM}. Thus, the common mode current I_{CM} is the major source of the scattered field for the transmission line. In the analysis of the scattering from the probe, the scattering from the dipole antenna and the transmission line will be evaluated separately and compared. As in the analysis of the reception by the probe, section III, the electromagnetic coupling between the dipole and the orthogonal transmission line is ignored.

The scattering cross ssections are convenient quantities for comparing the relative scattering from the dipole and transmission line and for studying the effect of parameters, such as the resistance per unit length of the transmission line, on the scattering. The cross sections considered are the total scattering cross section σ, which is the ratio of the total time-average power scattered P^s to the time-average power density of the incident wave S^i

$$\sigma(\theta_i, \phi_i; \psi_i) = P^s/S^i \ , \tag{35}$$

and the backscattering cross section σ_B, which is the ratio

$$\sigma_B(\theta_i,\phi_i;\psi_i) = P^s_{isotropic}/S^i \ , \tag{36}$$

where $P^s_{isotropic}$ is the total time-average power radiated by an isotropic scatterer that maintains the same electromagnetic field in all directions as maintained by the actual scatterer in the direction (θ_i,ϕ_i) toward the source [14]. The total scattering cross section in terms of the incident and scattered electric fields $\vec{E}^i$ and $\vec{E}^s$ is

$$\sigma(\theta_i,\phi_i;\psi_i) = \lim_{r\to\infty} \frac{\iint \vec{E}^s \cdot (\vec{E}^s)^* r^2 d\Omega}{\vec{E}^i \cdot (\vec{E}^i)^*} = \lim_{r\to\infty} \frac{\iint (|E_\theta{}^s|^2 + |E_\phi{}^s|^2) r^2 d\Omega}{|E^i|^2} \tag{37}$$

where $d\Omega$ is the element of solid angle for a sphere of radius r that completely encloses the scatterer. The backscattering cross sections considered are those for an incident wave broadside to the dipole or transmission line with the electric field parallel to the conductors. For the dipole antenna $(\theta_i = \pi/2,\ \phi_i = 0;\ \psi_i = 0)$

$$\sigma_{BA} = \sigma_B(\pi/2,0;0) = \lim_{r\to\infty} \frac{4\pi r^2 |E_\theta{}^s(\theta = \pi/2, \phi = 0)|^2}{|E^i|^2} \ , \tag{38}$$

and for the transmission line $(\theta_i = 0,\ \phi_i = \pi/2;\ \psi_i = 0)$

$$\sigma_{BL} = \sigma_B(0,\pi/2;0) = \lim_{r\to\infty} \frac{4\pi r^2 |E_\theta{}^s(\theta = 0, \phi = \pi/2)|^2}{|E^i|^2} \ . \tag{39}$$

When normalized to the square of the free-space wavelength λ_o, the well known cross sections for the electrically short dipole with its terminals short circuited $(Z_0 = 0)$ are [15], the total cross section

$$\sigma_A(\theta_i;\psi_i)/\lambda_o{}^2 = 2(\beta_o h)^6 \sin^2\theta_i \cos\psi_i / \{27\pi[\ell n(h/a_A) - 1]^2\} \ , \tag{40}$$

and the backscattering cross section

$$\sigma_{BA}/\lambda_o^2 = (\beta_o h)^6/\{9\pi[\ell n(h/a_A)-1]^2\} \ .^* \tag{41}$$

Before the cross sections for the transmission line can be evaluated, the common mode current distribution $I_{CM}(y)$ and the field that it produces $\vec{E}^s$ must be determined. The common mode current is a solution to the following approximate integral equation

$$2\pi \int_0^s \left[I_{CM}(y')e^{-j\beta_o R_e}/R_e\right]dy' - j2\pi \bar{z}^i \int_0^y I_{CM}(y')\sin \beta_o(y-y')dy'$$

$$= \frac{-j\beta_o E^i(\cos \psi_i \cos \theta_i \sin \phi_i + \sin \psi_i \cos \phi_i)}{\zeta_o(1 - \sin^2 \theta_i \sin^2 \phi_i)} e^{j\beta_o y \sin \theta_i \sin \phi_i}$$

$$+ A \cos \beta_o y + B \sin \beta_o y \ , \tag{42}$$

where A and B are constants to be determined by the end conditions $I_{CM}(0) = I_{CM}(s) = 0$, and the normalized internal impedance per unit length is

$$\bar{z}^i = z^i \lambda_o/\zeta_o \ . \tag{43}$$

This is the familiar integral equation for the current on a thin-wire scatterer with the equivalent radius

$$a_e = \sqrt{a_L b} \tag{44}$$

---

*These formulas differ from those of reference [15] in that the term $\ell n(4h/a_A)$ is replaced by $\ell n(h/a_A)$.

appearing in the distance R_e,

$$R_e = [(y-y')^2 + a_e^2]^{\frac{1}{2}} . \tag{45}$$

The equivalent radius approximately accounts for the fact that the transmission line is composed of two closely spaced conductors ($\beta_o b << 1$) carrying equal currents rather than a single conductor [16]. The integral equation (42) can be solved for the current by any of a number of straightforward numerical methods and the scattered field and cross sections determined [17]. Typical results are shown in Fig. 8 for the normalized total scattering cross section σ_L/λ_o^2 of a one wavelength long transmission line ($s = \lambda_o$, $a_e = 3.33 \times 10^{-3} \lambda_o$) with the incident field from the direction $\theta_i = 0$, $\phi_i = \pi/2$ and with the polarization $\psi_i = 0$ (E_θ^i component only). The cross section is shown as a function of the normalized internal resistance per unit length of the conductors $\bar{r}^i = r^i \lambda_o/\zeta_o$, and it is seen to be reduced significantly by an increase in the resistance once $\bar{r}^i$ is greater than about 10. The three regions marked on the graph represent typical ranges of σ_L/λ_o^2 at a frequency of 1 GHz for metallic wires with radius $a_L = 25$ μm (1 mil), the NBS carbon-Teflon conductor, and thin metallic film conductors. From this graph, it is clear why the high resistance transmission lines are often referred to as "transparent" to electromagnetic fields at high radio and microwave frequencies.

While numerical methods can provide an accurate solution to the integral equation (42) for specific values of the parameters, an analytic solution to the equation is more useful in performing parametric studies. An analytic expression for the current $I_{CM}(y)$ can be obtained by approximating the integral equation for the special case of interest, namely,

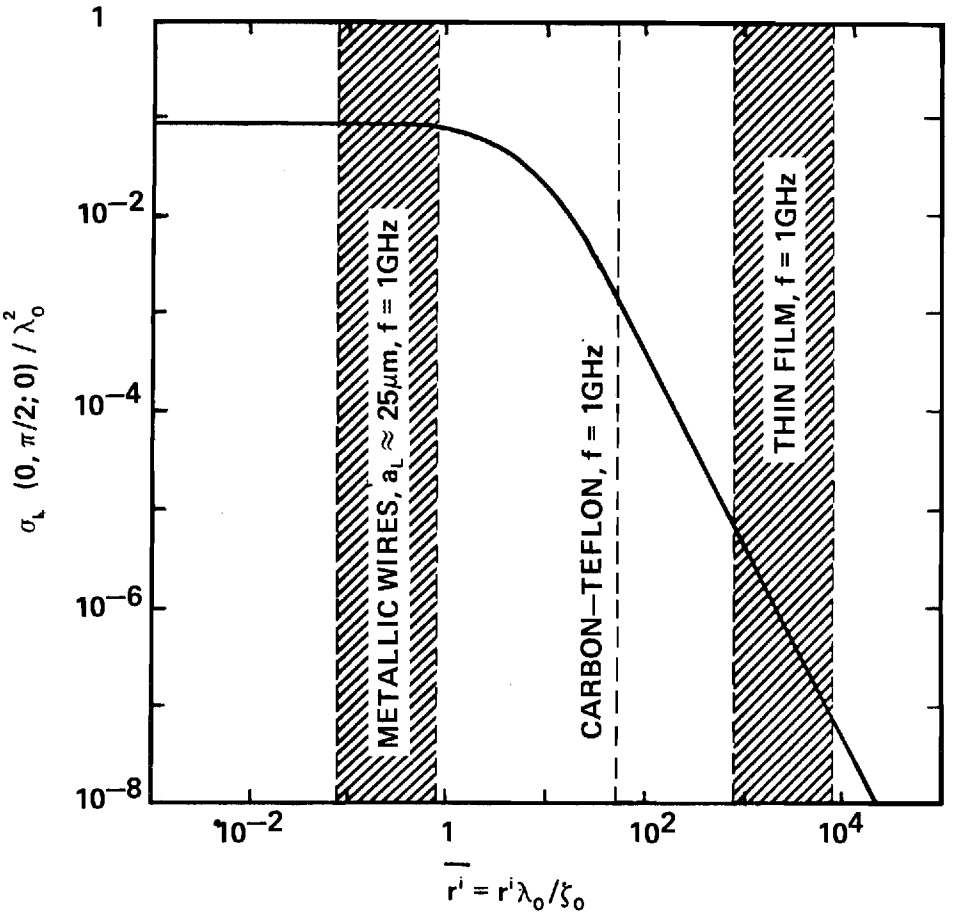

Figure 8. Normalized Total Scattering Cross Section of a One Wavelength Long Transmission Line ($s/\lambda_o = 1.0$, $a_e/\lambda_o = 3.33 \times 10^{-3}$) for an Incident Wave With $\theta_i = 0$, $\phi_i = \pi/2$ and $\psi_i = 0$.

conductors with a high internal impedance per unit length. The first integral on the left of (42) has a kernel with a sharp peak at the point y=y'. This behavior is often used in antenna theory to replace this integral by the term $2\pi\psi\ I_{CM}(y)$ and obtain the so-called "zeroeth-order" solution to the equation [16]. The particular choice of the constant ψ is not important for the purposes of the following argument, but an estimate of its magnitude can be obtained from the value for an electrically short antenna $\psi = 2\ell n(s/a_e)-2$. With this substitution, the approximate integral equation becomes

$$I_{CM}(y) - \frac{j\bar{z}^{i}}{\psi}\int_0^y I_{CM}(y')\sin\beta_o(y-y')dy' \approx$$

$$\frac{-jE^{i}\lambda_o(\cos\psi_i\cos\theta_i\sin\phi_i + \sin\psi_i\cos\phi_i)}{\zeta_o\psi(1-\sin^2\theta_i\sin^2\phi_i)}\ e^{j\beta_o y\sin\theta_i\sin\phi_i}$$

$$+ A'\cos\beta_o y + B'\sin\beta_o y\ . \qquad (46)$$

This is a Volterra integral equation of the second kind with a convolution-type kernel; its solution is easily obtained using the Laplace transformation [18],

$$I_{CM}(y) = \frac{-jE^{i}\lambda_o(\cos\theta_i\sin\phi_i\cos\psi_i + \cos\phi_i\sin\psi_i)}{\zeta_o\psi(1-\sin^2\theta_i\sin^2\phi_i - j\bar{z}^{i}/\psi)}\left\{e^{j\beta_o y\sin\theta_i\sin\phi_i}\right.$$

$$\left. - \left[\sin k_s(s-y) + \sin k_s y\ e^{j\beta_o s\sin\theta_i\sin\phi_i}\right]/\sin k_s s\right\}\ , \qquad (47)$$

where

$$k_s = \beta_s - j\alpha_s = \beta_o(1 - j\bar{z}^i/\psi)^{\frac{1}{2}} . \tag{48}$$

For the lossy transmission lines of interest, the resistance per unit length is high enough to make

$$|\bar{z}^i/\psi| = |z^i\lambda_o/\zeta_o\psi| >> 1 , \tag{49}$$

and

$$k_s \approx \beta_o\sqrt{\bar{z}^i/2\psi}\ (1-j) \tag{50}$$

In addition, the attenuation of a wave propagating along the length of the line s is large

$$\left| e^{-jk_s s} \right| = e^{-\alpha_s s} << 1 . \tag{51}$$

This last inequality follows from (22), since

$$\alpha_s s \approx \alpha_L s\sqrt{\psi\zeta_o/2\pi Z_{co}} , \tag{52}$$

where Z_{co} is the characteristic impedance of the transmission line when the conductors have zero internal impedance per unit length. The argument of the square root in (52) is usually of the order of unity; this can be seen by substituting the value of ψ for a short antenna and the value of Z_{co} for a two-wire transmission line

$$\psi\zeta_o/2\pi Z_{co} \approx [\ell n(s/a_e)-1]/\ell n(b/a_L) . \tag{53}$$

This ratio of logarithmic terms is usually less than five for practical geometries. Thus, when the inequality (22) applies to α_Ls, the inequality (52) for α_ss also holds. After using (49) and (51), the current (47) is approximately

$$I_{CM}(y) \simeq (E^i/z^i)(\cos\theta_i \sin\phi_i \cos\psi_i + \cos\theta_i \sin\psi_i)$$

$$\left\{ e^{j\beta_o y \sin\theta_i \sin\phi_i} - e^{-jk_s y} + e^{-jk_s(s-y)} e^{j\beta_o s \sin\theta_i \sin\phi_i} \right\}$$

$$\simeq (E^i/z^i)(\cos\theta_i \sin\phi_i \cos\psi_i + \cos\phi_i \sin\psi_i) e^{j\beta_o y \sin\theta_i \sin\phi_i} . \quad (54)$$

The last line in (54) is obtained by recognizing that terms with $-k_s$ in the exponent can be neglected, because they are only significant at points very close to the ends of the transmission line (y=0, s) when (51) is satisfied. Note, that to this degree of approximation, the current is independent of the parameter ψ.

The scattered electric field $\vec{E}^s$ in the far zone of the transmission line is

$$\vec{E}^s = -j\omega\mu_o(\hat{\theta}\cos\theta\sin\phi + \hat{\phi}\cos\phi)\frac{e^{-j\beta_o r}}{4\pi r}\int_0^s I_{CM}(y') e^{j\beta_o y' \sin\theta \sin\phi}\, dy' , \quad (55)$$

which, on substitution of (54) and evaluation of the integral, becomes

$$\vec{E}^s \simeq \frac{-4jE^i\lambda_o(\cos\theta_i \sin\phi_i \cos\psi_i + \cos\phi_i \sin\psi_i)\sin\left[\beta_o s(\sin\theta_i \sin\phi_i + \sin\theta \sin\phi)/2\right]}{\overline{z}_i\, 4\pi r(\sin\theta_i \sin\phi_i + \sin\theta \sin\phi)}$$

$$e^{-j\beta_o r} e^{j\beta_o s(\sin\theta_i \sin\phi_i + \sin\theta \sin\phi)/2}(\hat{\theta}\cos\theta\sin\phi + \hat{\phi}\cos\phi) . \quad (56)$$

The total scattering cross section σ_L and the backscattering cross section σ_{BL} for the transmission are obtained by using (56) in (37) and (39). After performing the surface integration in (37) and rearranging terms, the normalized total scattering cross section becomes

$$\sigma_L(\theta_i,\phi_i,\psi_i)/\lambda_o^2 \approx (2/\pi|\bar{z}^i|^2)|\cos\theta_i \sin\phi_i \cos\psi_i + \cos\theta_i \sin\psi_i|^2$$

$$\Big[(1/\beta_o s)\sin\beta_o s \cos(\beta_o s \sin\theta_i \sin\phi_i) - 2$$

$$+ \sin\theta_i \sin\phi_i \sin\beta_o s \sin(\beta_o s \sin\theta_i \sin\phi_i)$$

$$+ \cos\beta_o s \cos(\beta_o s \sin\theta_i \sin\phi_i)$$

$$+ \sin\theta_i \sin\phi_i \{\mathrm{Cin}[\beta_o s(1 + \sin\theta_i \sin\phi_i)] - \mathrm{Cin}[\beta_o s(1 - \sin\theta_i \sin\phi_i)]\}$$

$$+ (\beta_o s/2)(1 - \sin^2\theta_i \sin^2\phi_i)\{\mathrm{si}[\beta_o s(\sin\theta_i \sin\phi_i + 1)]$$

$$- \mathrm{si}[\beta_o s(\sin\theta_i \sin\phi_i - 1)]\}\Big] \quad , \tag{57}$$

where si(x) and Cin(x) are the sine and cosine integrals [19]

$$\mathrm{si}(x) = \mathrm{Si}(x) - \pi/2 = -\int_0^{\pi/2} e^{-x\cos t} \cos(x \sin t)dt \quad , \tag{58}$$

$$\mathrm{Cin}(x) = -\mathrm{Ci}(x) + \ell n(x) + \gamma = -\int_0^x (\cos t - 1)/t \, dt \quad , \tag{59}$$

and γ is Euler's constant. The normalized backscattering cross section is simply

$$\sigma_{BL}/\lambda_o^2 \simeq (\beta_o s/|\bar{z}^i|)^2/\pi = [\beta_o s/(|\bar{z}^i|\lambda_o/\zeta_o)]^2/\pi \ . \qquad (60)$$

The normalized total scattering cross section $(\sigma_L/\lambda_o^2)/(\beta_o s/|\bar{z}^i|^2)$ computed from (57) is shown in Fig. 9 as a function of the electrical length $\beta_o s$ of the transmission line. The incident wave for this example is in the plane $\phi_i = \pi/2$ with the electric field in the direction $\hat{\theta}_i$ ($\psi_i = 0$); the angle θ_i is the parameter on the graph. This orientation and polarization for the incident wave provides a complete description of the scattering, since the scattering by the line is rotationally symmetric about the y axis as a result of approximating the two conductors of the line by one of equivalent radius, and only the component of the incident electric field that is parallel to the y axis is scattered by the line. Two sets of cross sections computed from the numerical solution of the integral equation (42) are also shown in Fig. 9. These are for an angle of incidence $\theta_i = 0$ and two values of the normalized resistance per unit length, $|\bar{r}^i|/\psi = 10$, 100, where ψ is taken to be $\psi = 2\ell n(s/a_e)-2$. As expected, the total scattering cross sections obtained using the approximate formula (57) are in good agreement with those from the numerical analysis when the parameter $|\bar{r}^i|/\psi$ is large.

The maximum cross section for any of the lengths $\beta_o s$ shown in Fig. 9 occurs when the angle of incidence is $\theta_i = 0$,

$$\sigma_L(0,\pi/2;0)/\lambda_o^2 = (2/\pi|\bar{z}^i|^2)[(1/\beta_o s)\sin \beta_o s - 2$$

$$+ \cos \beta_o s + \beta_o s \ \mathrm{Si}(\beta_o s)] \ . \qquad (61)$$

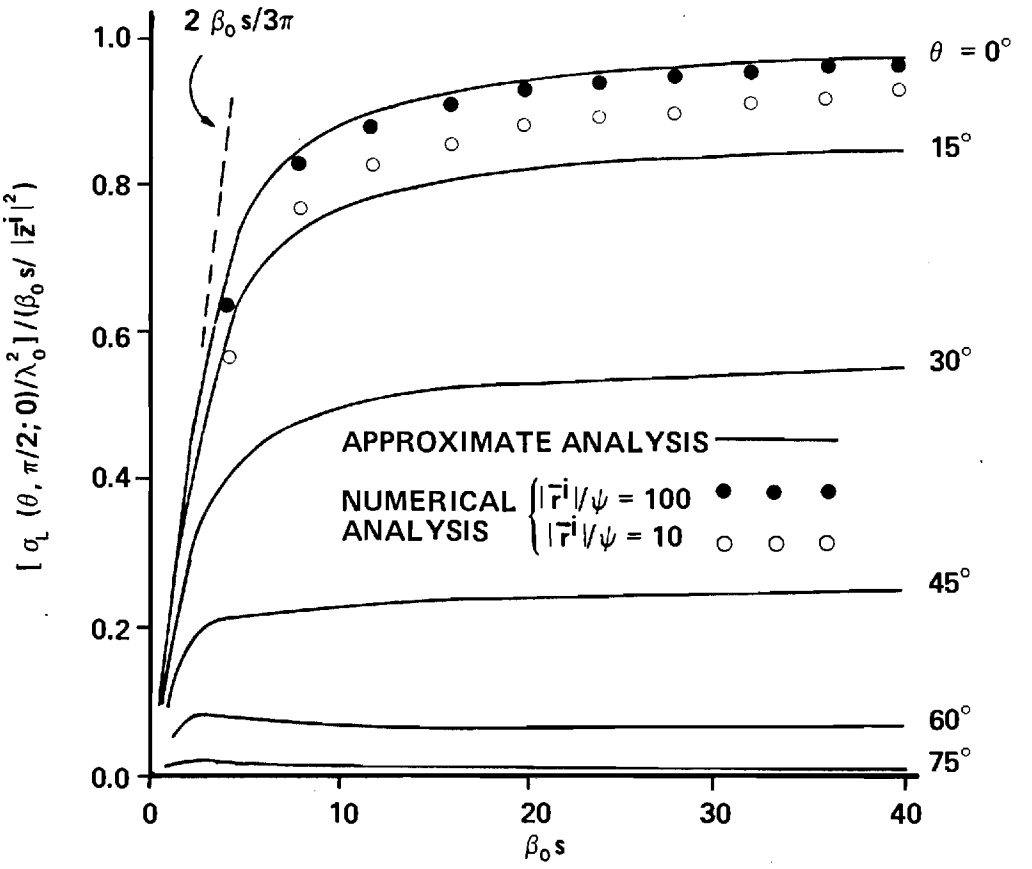

Figure 9. Normalized Total Scattering Cross Section for Transmission Line as a Function of the Electrical Length β_0 s, $\phi_i = \pi/2$, $\psi_i = 0$.

For electrically short lines $\beta_o s << 1$, the total cross section is approximately

$$\sigma_L(0,\pi/2;0)/\lambda_o^2 \approx 2(\beta_o s)^2/(3\pi|\bar{z}^i|^2) , \tag{62}$$

and for electrically long lines $\beta_o s >> 1$, the total cross section approaches

$$\sigma_L(0,\pi/2;0)/\lambda_o^2 \sim \beta_o s/|\bar{z}^i|^2 , \tag{63}$$

see Fig. 9. The asymptotic value given in (63) is useful as an upper bound for the total scattering cross section of the lossy transmission line for all angles of incidence and polarizations of the incident wave.

The approximate formulas for the cross sections (57), (60), (62) and (63) can be used to study the effect of various parameters, such as the resistance per unit length r^i and the frequency, on the scattering by the lossy transmission line. A relative measure of the scattering is obtained by comparing these cross sections with those for the dipole antenna in the probe, (40) and (41). For example, a comparison can be made of the total scattering from the dipole and from a length of the transmission line equal to the length of the dipole, i.e., the ratio $(\sigma_L/s)/(\sigma_A/2h)$. If the maximum values of the total cross section for the line (61) and for the dipole, (40) with $\theta_i = \pi/2$, $\psi_i = 0$, are used, this ratio becomes

$$\frac{\sigma_L(0,\pi/2;0)/s}{\sigma_A(\pi/2;0)/2h} = \frac{54(h/s)}{|\bar{z}^i|^2(\beta_o h)^6}\left[(1/\beta_o s)\sin\beta_o s - 2\right.$$

$$\left. + \cos\beta_o s + \beta_o s\,\mathrm{Si}(\beta_o s)\right]\left[\ell n(h/a_A) - 1\right]^2 . \tag{64}$$

For an internal impedance per unit length that is approximately a frequency independent resistance $z^i \approx r^i$, the right side of (64) is inversely proportional to the square of the frequency when the line is electrically short ($\beta_o s << 1$), and inversely proportional to the cube of the frequency when the line is electrically long ($\beta_o s >> 1$).

V. THE TRANSMISSION LINE AS A LOW-PASS FILTER

The highly resistive transmission lines used in miniature field probes are very dispersive, i.e., the phase velocity for a wave propagating on the line is a strong function of the frequency. This is illustrated in Fig. 10 where the voltage transmission ratio

$$V(s) \; / \; V(0) \;\; = \sec(k_L s) \tag{65}$$

for a transmission line terminated in an open circuit, $Z_s = \infty$, is graphed as a function of the frequency. Results are shown for 20 cm long lines formed from carbon-Teflon conductors (r^i = 65.6 kΩ/m) and thin film conductors (r^i = 10 MΩ/m); the capacitance per unit length of both lines is c = 20 pF/m. The transmission ratio is seen to drop sharply once the frequency exceeds the point where $|k_L s| = 1$. For the carbon-Teflon conductors this occurs at about f = 10 MHz and for the thin-film conductors at about f = 10 kHz.

Consider a probe, like that shown in Fig. 1, which is to measure amplitude modulated incident electric fields of the form

$$\vec{E}^i(\vec{r},t) = \vec{E}^i(\vec{r})\; f(t)\; \cos(\omega_o t + \phi(\vec{r})) \; . \tag{66}$$

The modulating signal f(t) in (66) is band limited, i.e., its Fourier transform F(ω) is zero above the frequency ω_m,

$$F(\omega) = 0 \; , \qquad |\omega| > \omega_m \; . \tag{67}$$

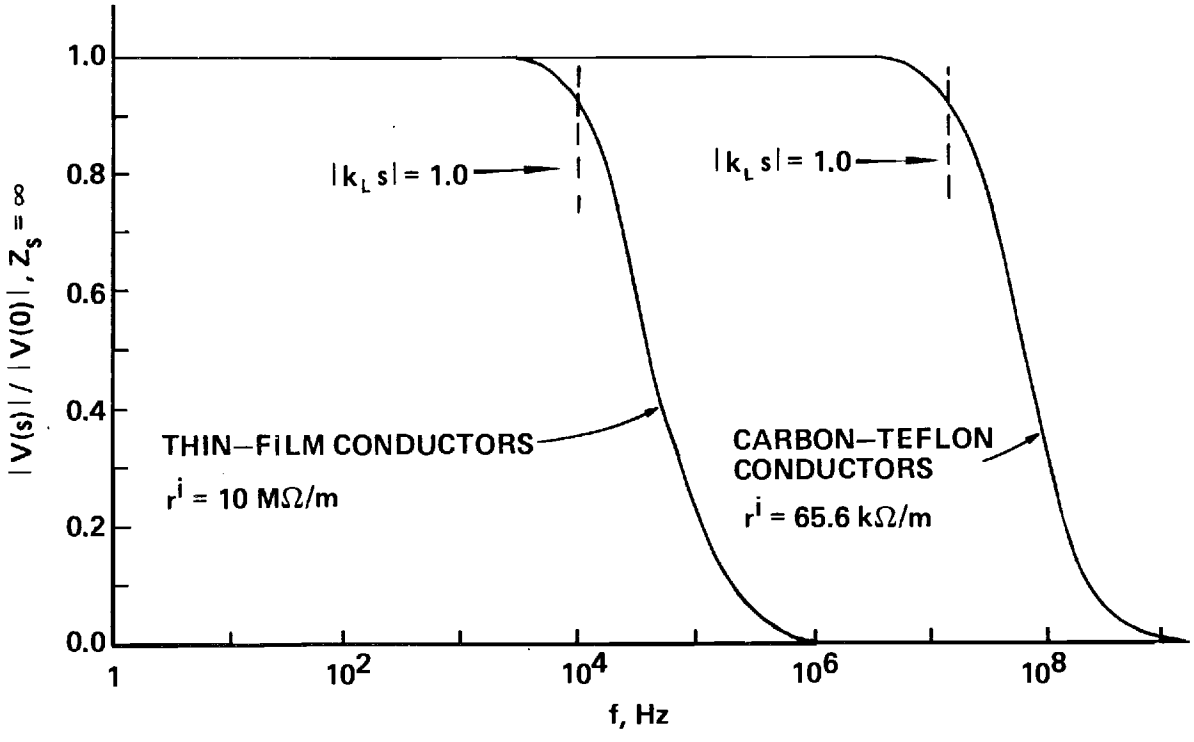

Figure 10. The Voltage Ratio $|V(s)| / |V(0)|$ as a Function of Frequency for Resistive Transmission Lines Terminated in an Open Circuit, $Z_s = \infty$.

The dipole antenna of the probe receives the incident signal (66) and impresses a voltage proportional to it across the diode. The nonlinear characteristic of the diode produces a current $i_d(t)$ proportional to the square of the amplitude modulation on the incident signal,

$$i_d(t) = C\left|f(t)\right|^2 \quad . \tag{68}$$

The Fourier transform of this current $I_d(\omega)$ is also band limited

$$I_d(\omega) = 0 \quad , \qquad \left|\omega\right| > 2\omega_m \quad . \tag{69}$$

For the transmission line to pass this current to the monitoring instrumentation without distortion, the frequency $2\omega_m$ must be below the frequency where $\left|k_L(\omega)s\right| = 1$. As discussed earlier the inequality $\left|k_L(\omega_o)s\right| >> 1$ must be satisfied at the high radio or microwave carrier frequency ω_o to minimize the perturbation in the reception produced by the transmission line. Thus, with reference to Fig. 10, for proper operation of the probe the carrier frequency ω_o of the incident signal must be well above the point where $\left|k_L s\right| = 1.0$, while the frequencies contained in the square of the modulating signal ($\omega \leq 2\omega_m$) must be below this point.

When the parameters for the transmission line and the modulation are selected so that the inequality

$$\left|k_L(\omega)s\right|^2 \approx \omega c 2 r i s^2 << 1 \tag{70}$$

is satisfied at the frequencies $\omega \leq 2\omega_m$, the resistive transmission line can be represented by the equivalent "Pi" network shown in Fig. 11. The

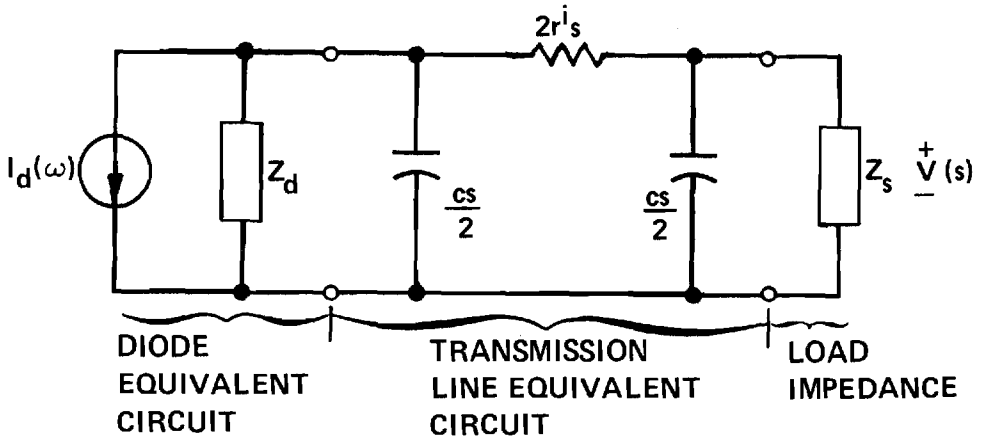

Figure 11. Low-Frequency Output Circuit for Diode, Transmission Line and Termination, Z_s.

other elements in this circuit diagram are the low-frequency Norton equivalent circuit for the output of the diode and the input impedance of the monitoring instrumentation Z_s. In the diode equivalent circuit $I_d(\omega)$ is the short circuit output current and Z_d the diode "video impedance," often taken to be a resistance, viz, R_v the video resistance.* An expression for the voltage V(s) at the input to the monitoring instrumentation is obtained from the equivalent circuit in Fig. 11. When the inequality (70) is used to simplify this expression, the voltage is approximately

$$V(s) \approx -I_d Z_s Z_d/(Z_d + Z_s + 2r^i s + j\omega cs\ Z_d Z_s)$$

$$= -I_d Z_s Z_d/\{2r^i s(1 + Z_d/2r^i s) + Z_s[1 - j(k_L s)^2(Z_d/2r^i s)]\} \ . \qquad (71)$$

For a practical probe, the resistance of the transmission line $2r^i s$ is usually much greater than the diode impedance,

$$|Z_d/2r^i s| << 1 \ . \qquad (72)$$

After using the inequalities (70) and (72), (71) becomes

$$V(s) \approx -I_d Z_s Z_d/[2r^i s + Z_s] \ . \qquad (73)$$

To sumarize the results of this section, the resistive transmission line in the field probe behaves as a low-pass filter. If the probe is to be

---

*The details of the equivalent circuit for the diode and its use in the equivalent circuit for the field probe are given in Chapter 3 of reference [10].

used to measure an amplitude modulated field without distortion, the frequencies in the square of the modulating signal must lie within the passband of the transmission line, i.e., (70) must be satisfied for all frequencies $\omega \leq 2\omega_m$. The voltage across the input impedance Z_s of the monitoring instrumentation is then simply determined from (71) or (73).

VI. COMPARISON WITH EXPERIMENT

The previously obtained theoretical results show that the transmission line with finite resistance will distort the field pattern of the electric field probe from that of an ideal electrically short dipole. To verify these results, a model probe was constructed with the dimensions h = 1.25 cm, b = 5.0 mm, a_A = 0.19 mm, a_L = 0.38 mm, and s = 15.0 cm. The conductors of the resistive transmission line were the NBS designed carbon-Teflon filament, r^i = 65.6 kΩ/m. At the frequency used for the measurements, f = 800 MHz, the inequality (22) was satisfied, $e^{-\alpha_L s}$ = 1.8×10^{-3}, making the reception by the probe independent of the length of the transmission line and load impedance Z_s.

The probe was placed in an approximately plane electromagnetic wave with electric field $\vec{E}_\theta{}^i$ in the plane formed by the dipole and transmission line ($\phi_i = \pi/2, 3\pi/2$), see Fig. 12a. A field pattern was obtained by monitoring the signal at the end of the transmission line as the probe was rotated about the x axis to vary the angle θ_i. Data were taken on both sides of the plane of symmetry for the probe ($\theta_i = \pi/2$) and averaged to produce a single pattern. The system was calibrated to be certain that the diode was operating in the square-law region over the range of measurement. The measured and theoretical field patterns are compared in Fig. 13a, and they are seen to be in good agreement. Note that the position of the null in the pattern is shifted from $\theta_i = 0$, the point where it would occur for an ideal electrically-short dipole with the pattern $|\sin \theta_i|$. This shift is about 5° which agrees well with the predictions of the theory (34).

In this example, the distortion of the field pattern by the resistive transmission line was minor. To test the theory further, a highly-

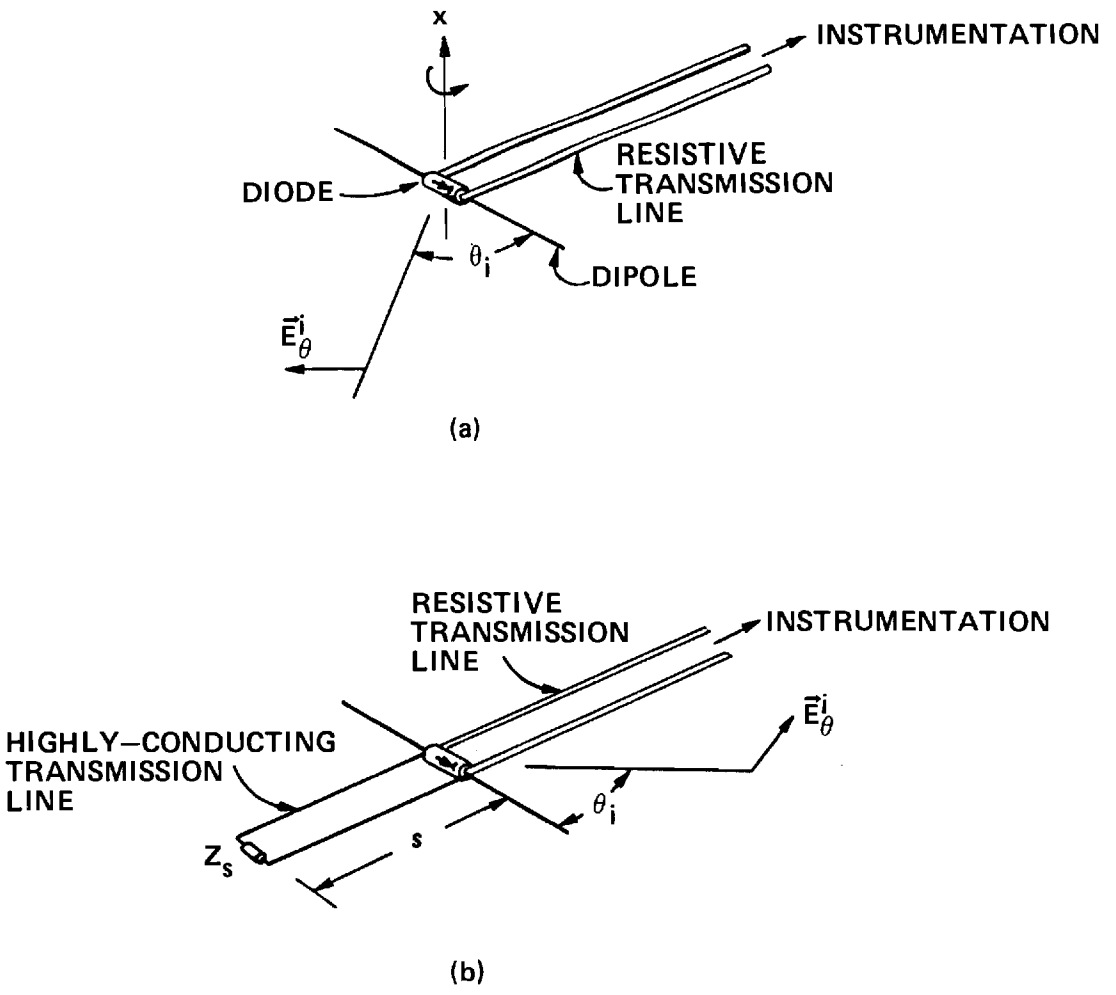

Figure 12. Detail of Experimental Probe
(a) With Resistive Transmission Line
(b) With Highly-Conducting and Resistive Transmission Lines.

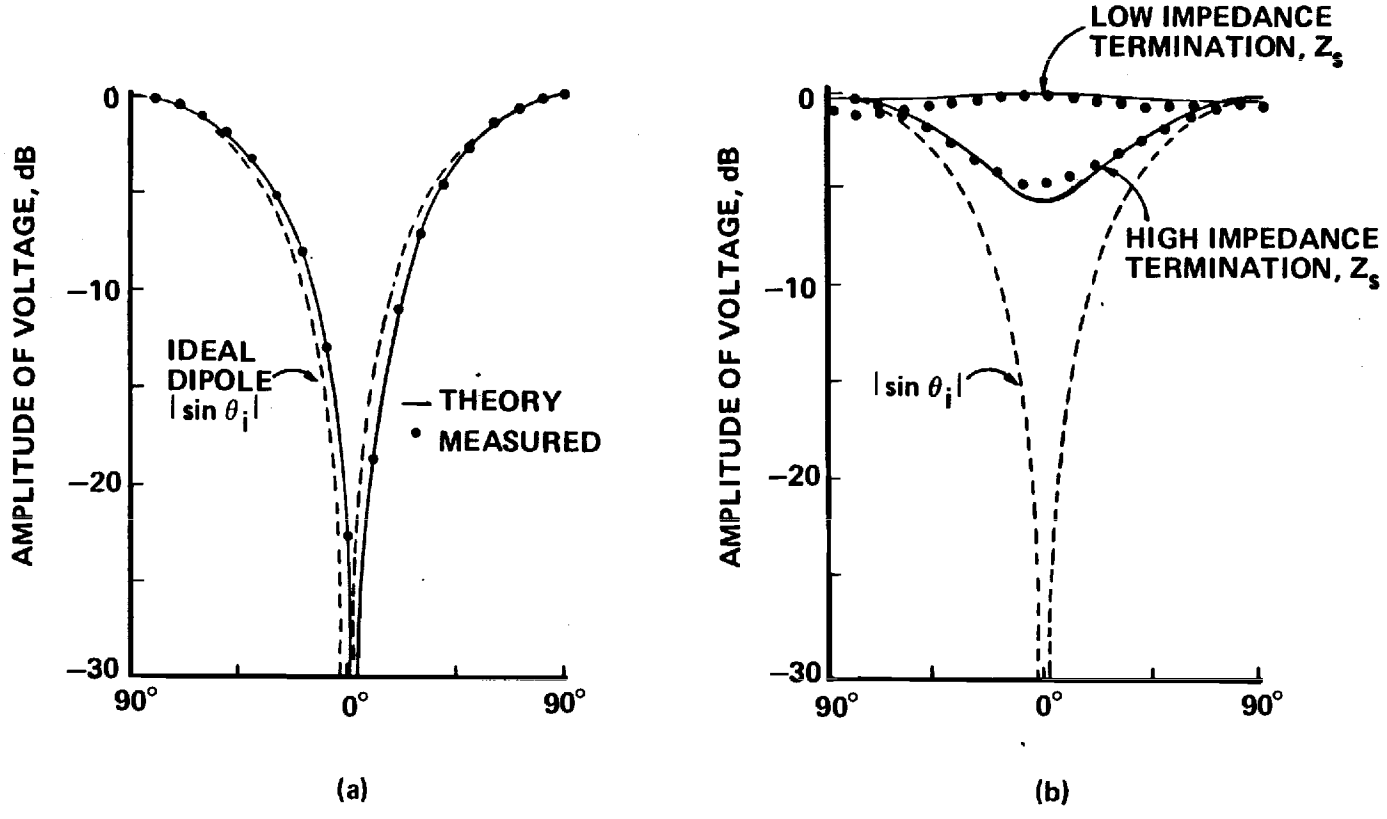

Figure 13. Comparison of Measured and Theoretical Field Patterns in Plane $\phi_i = \pi/2, 3\pi/2$ With Incident Field $\vec{E}^i_\theta$

(a) Highly Resistive Transmission Line
(b) Highly–Conducting Transmission Line.

conducting transmission line was used with the probe. The conductors of the line were copper with the dimensions a_L = 0.32 mm and s = 7.0 cm. At the high frequency used in this experiment, it is difficult to terminate the highly-conducting parallel-wire transmission line in a known impedance and to precisely measure the voltage across that impedance without interfering with the reception of the incident signal by the dipole. To overcome this difficulty, the highly-conducting transmission line was placed in parallel with the resistive transmission line already described, see Fig. 12b. Since the resistive line was shown to have a minor effect on the field pattern of the probe, the pattern measured in this manner is approximately that of the dipole with the highly-conducting transmission line.

Field patterns were measured with the highly-conducting transmission line terminated in two different impedances Z_s: an open circuit and a low impedance formed by a lumped capacitor, $|Z_s/Z_c| \approx 0.17$. These patterns are compared with the theoretical results in Fig. 13b, and they are seen to be in good agreement. Note that the theoretical results for the highly conducting transmission line were computed from the general expression (19), which is a function of the length of the line s and load impedance Z_s.

A comparison of Figures 13a and 13b shows the great improvement in the field pattern of the probe obtained by replacing a highly conducting transmision line with a highly resistive one.

VII. SUMMARY AND CONCLUSIONS

The electric field probe with the configuration shown in Fig. 1 has been analyzed to determine the effect of the lossy transmission line on its performance. The following conclusions can be drawn from the analysis.

i. The reception of the incident field by the transmission line distorts the field pattern of the probe from that of an ideal electrically short dipole antenna. For a highly resistive transmission line, the distortion of the pattern is proportional to the parameter χ (31); this includes the distortion that is the reception of a signal polarized so it will not be received directly by the dipole. In the design of a field probe, this parameter is useful for comparing the distortion produced by different line geometries.

ii. The scattering of the incident field by the transmission line was shown to be greatly reduced by making the conductors highly resistive; thus, the reason for referring to such lines as "transparent." The simple expressions developed for the total scattering cross section and the backscattering cross section of the highly resistive line (57)-(63) can be used to obtain a relative measure of the scattering from different line geometries and for comparing the scattering from the line with that from the dipole.

iii. The highly resistive transmission line behaves as a low-pass filter. If the probe is used to measure amplitude modulated signals, the significant frequencies in the square of the modulating signal must be within the pass band of this fil-

ter. For practical probes this will be true when the highest frequency f_m in the band-limited modulating signal satisfies the inequality $f_m << (8\pi\ cr^i s^2)^{-1}$.

To illustrate the use of these results, consider the miniature field probe in Fig. 14, recently developed by the U.S. Bureau of Radiological Health (BRH) for the measurement of amplitude modulated fields with carrier frequencies in the range 0.2 to 12 GHz and modulating signals with frequency content in the range $0 \leq f \leq 2$ kHz [6]. The parameters for this probe were selected empirically. The dipole antenna is formed from a flat strip of half length h = 1.25 mm and width w = 50 μm; this strip is equivalent to a round conductor with a radius $a_A \simeq w/4 = 13\ \mu m$ [16]. The conductors of the high resistance transmission line are of length s = 6.5 cm and spacing b = 50 μm. The resistance per unit length of the thin film conductors is $r^i \simeq 9.7$ MΩ/m, and the capacitance per unit length of the transmission line is $c \simeq 57$ pF/m. This transmission line is extremely lossy at the frequencies in the range of measurement; the exponential in (22) being $e^{-\alpha_L s} \leq e^{-54}$. The parameter χ (31) is very small, $\chi = 7.1 \times 10^{-4}$; thus, the distortion of the field pattern due to the transmission line is negligible. The theoretical shift in the nulls of the dipole pattern (34) is only $\Delta\theta \simeq 0.04^o$.

The normalized total scattering cross section for the transmission line $\sigma_L(0,\pi/2;0)/\lambda_o^2$ is determined approximately by the small argument formula (62) at the lowest frequency 0.2 GHz ($\beta_o s = 0.27$) and by the asymptotic value (63) at the highest frequency 12 GHz ($\beta_o s = 16.3$). The ratio of the total scattering cross section per unit length of the transmission line to that for the dipole antenna $[\sigma_L(0,\pi/2;0)/s]/[\sigma_A(\pi/2;0)/2h]$ decreases from 10^4 at 0.2 GHz to 0.86 at 12 GHz.

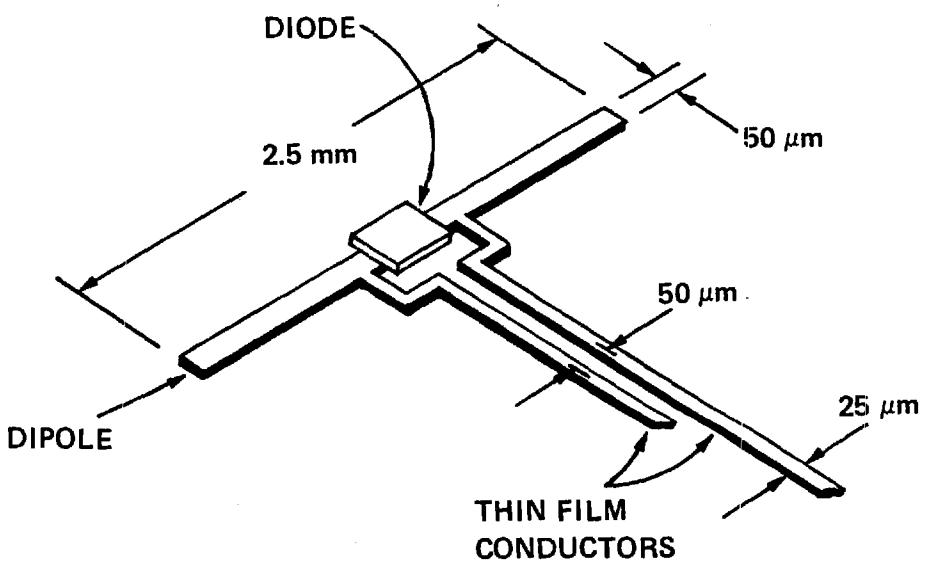

Figure 14. Detail of BRH Probe.

The quantity $|k_L(\omega)s|^2$ (71) is equal to one at the frequency f = 34 kHz; thus, a field can be measured with little distortion when the maximum frequency in the amplitude modulation is $f_m \ll 17$ kHz. This requirement is well satisfied when the probe is used within specifications, $f_m = 2$ kHz.

ACKNOWLEDGMENTS

The author wishes to thank Dr. T. Batchman of the University of Virginia and Mr. H. Bassen of the Bureau of Radiological Health for their helpful comments on the work presented in this paper.

REFERENCES

[1] C. L. Andrews, "Diffraction Pattern in a Circular Aperture Measured in the Microwave Region," J. Appl. Phys., vol. 21, pp.761-767, Aug. 1950.

[2] A. W. Rudge, "An Electromagnetic Radiation Probe for Near-Field Measurements at Microwave Frequencies," Journal of Microwave Power, vol. 5, pp. 155-174, Nov. 1970.

[3] F. Greene, "Development of Electric and Magnetic Near Field Probes," N.B.S. Tech. Note 658, Jan. 1975.

[4] R. R. Bowman, "Some Recent Developments in the Characterization and Measurement of Hazardous Electromagnetic Fields," Biological Effects and Health Hazards of Microwave Radiation, Warsaw, Poland: Polish Medical Publishers, 1974, pp. 217-227.

[5] H. Bassen, M. Swicord, and J. Abita, "A Miniature Broad-Band Electric Field Probe," Annals of the New York Academy of Sciences, Biological Effects of Nonionizing Radiation, vol. 297, pp. 481-493, Feb. 1975.

[6] H. Bassen, W. Herman, and R. Hoss, "EM Probe with Fiber Optic Telemetry," Microwave J., vol. 20, pp. 35-39, Apr. 1977.

[7] H. Bassen, P. Herchenroeder, A. Cheung, and S. Neuder, "Evaluation of an Implantable Electric-Field Probe Within Finite Simulated Tissues," Radio Sci., vol. 12, pp. 15-25, Nov.-Dec. 1977.

[8] G. S. Smith, "A Comparison of Electrically Short Bare and Insulated Probes for Measuring the Local Radio Frequency Electric Field in Biological Systems," IEEE Trans. Biomed. Eng., vol. BME-22, pp. 477-483, Nov. 1975.

[9] G. S. Smith, "The Electric-Field Probe Near a Material Interface with Application to the Probing of Fields in Biological Bodies," IEEE Trans. Microwave Theory Tech., vol. MTT-27, pp. 270-278, March 1979.

[10] R. W. P. King and G. S. Smith, Antennas in Matter: Fundamentals, Theory and Applications. Cambridge, MA: M.I.T. Press, 1981, Ch. 3.

[11] S. H. Mousavinezhad, K.-M. Chen, and P. Nyquist, "Response of Insulated Electric Field Probes in Finite Heterogeneous Biological Bodies," IEEE Trans. Microwave Theory and Techniques, vol. MTT-26, pp. 599-607, Aug. 1978.

[12] C. D. Taylor, R. S. Saterwhite, and C. W. Harrison, Jr., "The Response of a Terminated Two-Wire Transmission Line Excited by a Non uniform Electromagnetic Field," IEEE Trans. Antennas Propagat., vol. AP-13, pp. 987-989, Nov. 1965.

[13] A. A. Smith, Jr., Coupling of External Electromagnetic Fields to Transmission Lines. New York: Wiley-Interscience, 1977.

[14] R. W. P. King ad T. T. Wu, The Scattering and Diffraction of Waves. Cambridge, MA: Harvard University Press, 1959.

[15] J. H. Van Vleck, F. Bloch, and M. Hamermesh, "Theory of Radar Reflection from Wires or Thin Metallic Strips," J. Appl. Phys., vol. 18, pp. 274-294, March 1947.

[16] R. W. P. King, The Theory of Linear Antennas. Cambridge, MA: Harvard Univ. Press, 1956.

[17] R. F. Harrington, Field Computations by Moment Methods. New York: Macmillan, 1968.

[18] F. G. Tricomi, Integral Equations. New York: Wiley-Interscience, 1957.

[19] M. Abramowitz and I. A. Stegun, Handbook of Mathematical Functions. Washington, D.C.: U.S. Government Printing Office, 1964.